DEPOSITIONAL RELATIONSHIP BETWEEN CARBONATE AND CLASTIC ENVIRONMENTS OF THE EARLY PERMIAN LABORCITA FORMATION NEAR TULAROSA, NEW MEXICO

by

Bruce Mitchell Rundell

Submitted in Partial Fulfillment
of the Requirements for the Degree of
Master of Science in Geology

NEW MEXICO INSTITUTE OF MINING AND TECHNOLOGY

Socorro, New Mexico

June, 1982

TABLE OF CONTENTS

ACKNOWLEDGMENTS

I would like at this time to thank my parents for their moral and financial support during this study. Kathy Rider, David Wingo, Alan Carmichael and Clay Melton for their assistance in the surveying of the area, New Mexico Bureau of Mines drafting department for their help, the New Mexico Geologic Society for their financial support and last but not least Dr. Dave Johnson, Dr. John MacMillan and Dr. Clay Smith for their guidance and advice during this investigation.

Abstract

The depositional relationship between clastic and arbonate sediments of the Laborcita Formation, near Tularosa, New Mexico was caused by periodic changes in the irection and volume of clastic influx onto the Oro Grande helf. Within this area, clastic sediments were restricted to deposition on a fan-delta and shoreface, while carbonate sediments were deposited on a shelf and within lagoons and interdistributary bays.

Decreases in clastic influx, subsidence of underlying strata, and tectonic movement allowed clastic deposition to be replaced shelf conditions. During some of these periods bioherms were formed on the shallow shelf. This occurred twice during the deposition of the Laborcita Formation within the study area. Undulating brownish-gray and light-gray color zones formed within the massive bioherm core. These represent stages in the development of the bioherm. The lower brownish-gray zone formed during the growth stage, when phylloid algal plates were piled up by wave action in a transgressing sea. The growth of the bioherm was unable to keep up with the increase in depth, due to the decrease in light penetration. With the absence of profuse algal production the growth stage ended and the bioherm was inhabited by bryozoans, crinoids, brachiopods, p ecypods, gastropods, and foraminifera. This represe- the colonizing stage seen in the light-gray zone. B

velopment alternated between these stages three times. Along the top of the bioherm wavy, parallel bedding occurs. These beds drape the upper surface of the bioherm core, and represent flanking and overlying lagoonal beds. The occurrence of lagoonal beds at the top of the sequence indicates progradation of the bioherm complex.

Development of the bioherm ended with the return of clastic material into the environment. This is seen by the presence of prodelta shales onlapping the back of the bioherm. Reestablishment of the fan-delta never occurred in this area, and clastics were deposited along the shoreface.

Another bioherm developed at the top of the Laborcita Formation. Development of this bioherm was not as great as the previous one. This is due either to the influence of prograding terrigenous Abo sands or the lack of preservation of the main body of the bioherm.

Below the main bioherm a ledge-forming, continuous carbonate unit is interpretated to be a lagoonal deposit. This interpretation predicts the presence of a bioherm to the west in the subsurface.

LIST OF FIGURES

INTRODUCTION

The depositional relationship between marine carbonates and terrigenous sediments has not been emphasized in previous work. Much work has been done on each individually, but little has been done relating them to each other. The lateral contact between these two environments may occur along one of three types of shoreline: 1) linear clastic shoreline, where the sediments grade basinward from terrigenous sandstones and conglomerates to shallow nearshore siltstones and mudstones, and finally into marine carbonates; 2) barrier shorelines, where terrigenous sediments are restricted to the barrier complex allowing the deposition of carbonates basinward of the barrier; and 3) deltaic complexes, where terrigenous sediments are restricted to meandering deltaic channels and delta flats with carbonate deposition basinward. The shape and size of delta complexes varies according to the amount of terrigenous debris and the intensity of wave action on the delta front. Each of these types of environments may occur along a given shoreline at different times in its geologic history with or without deposition of carbonate material.

The Lower Permian upper Laborcita Formation (Otte, 1959) of the Northern Sacramento Mountains of New Mexico contains an area where such an investigation may be conducted. This area, T 14 S, R 10 E, section 16, is located on the Mescalero 15 minute quadrangle, Otero County

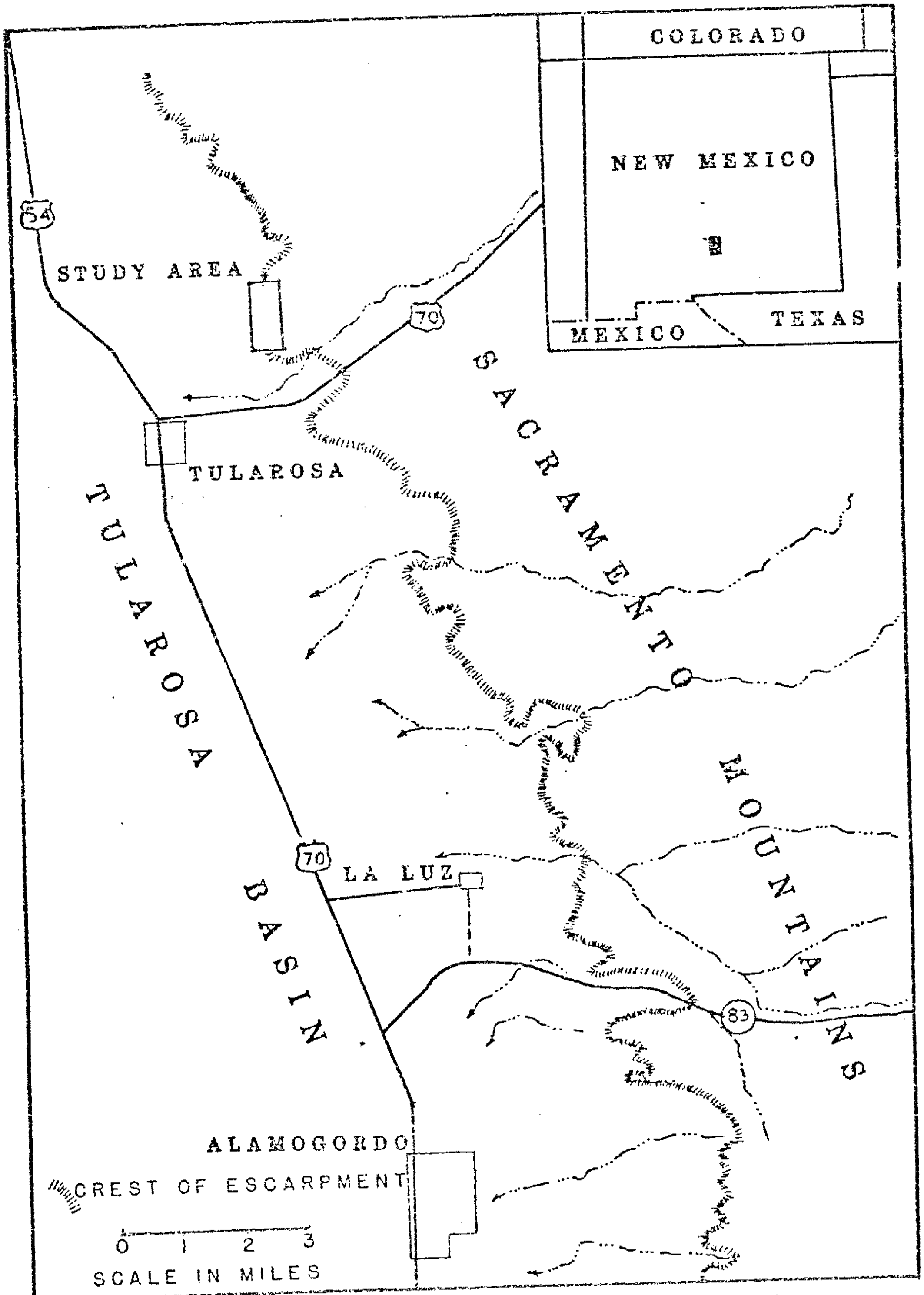

Fig. 1. Index map showing location of study area, near Tularosa, New Mexico.

and is readily accessible by taking County Road B18 and B19 east off of U.S. Highway 54, approximately one mile (1.6 km) north of the town of Tularosa (Fig. 1).

The area consists of the lower bluff or escarpment of the Sacramento Mountains (Fig. 2). The climate of the area is a hot desert, with summer thunderstorms and dry winters. This gives rise to an area of relatively good exposure. Ocotillo, mescal, cholla, prickly pear and mesquite are found in this area. The bluff makes the area ideal for birds of prey, which thrive on the abundant population of jackrabbits and other rodents.

First mapped by Otte (1959) as part of a doctoral dissertation on the stratigraphy of the Late Pennsylvanian and Early Permian, the area is noted for vertical cycles and lateral transitions from open marine to terrestrial flood plain environments. Of particular interest is a bioherm, which occurs near the middle of this sequence. Fabric studies by Otte and Parks (1963) investigated the origin of the black and white crystalline calcite mosaic within the bioherm core. This was followed by study of the community succession within the bioherm by Toomey and Cys (1979). Both of these discussions focused on the bioherm, with little attention given to the larger-scale depositional environment in which it formed and its relationship to the clastic sediment in the area.

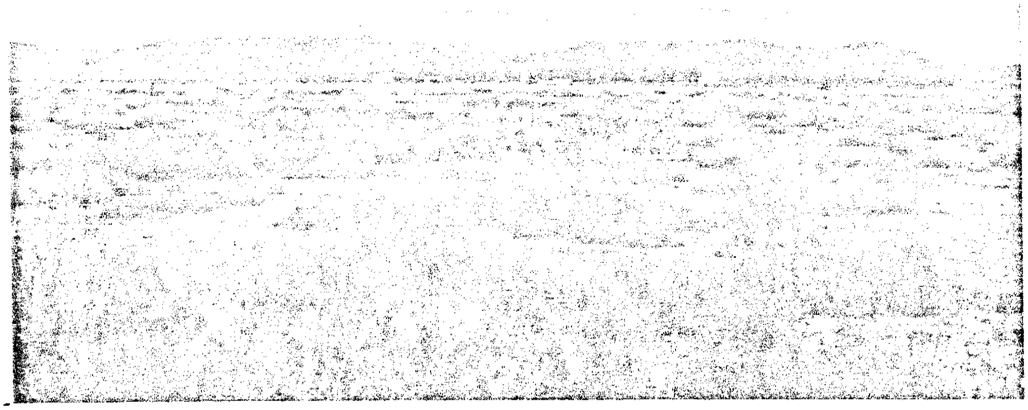

Fig. 2. Photo of Sacramento escarpment and study area.

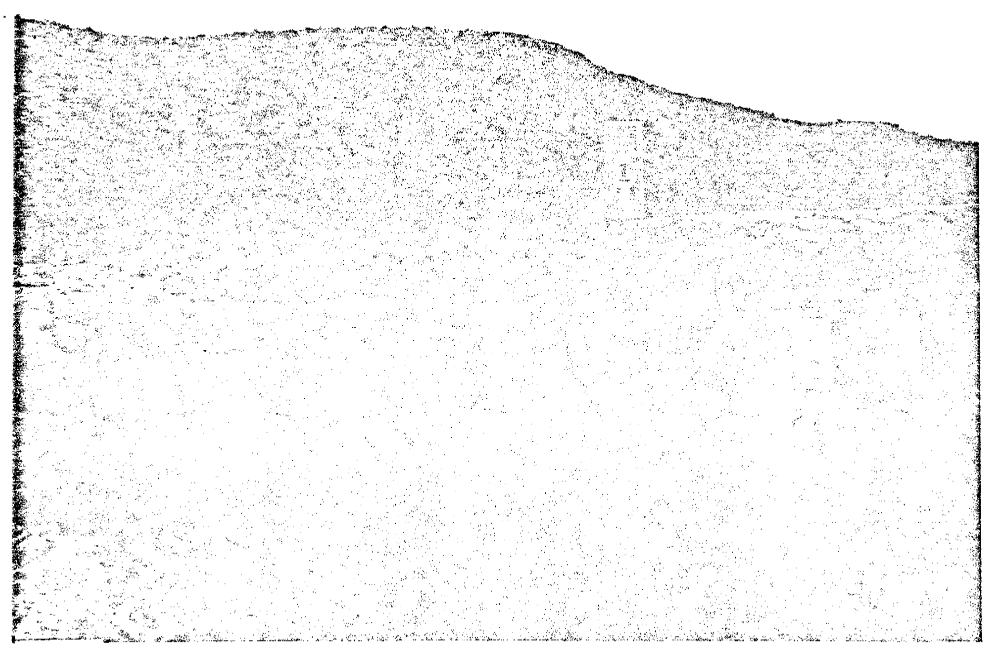

Fig. 3. Photo showing trough-shaped bedding change (at arrow 1) and gradational color change (at arrow 2).

To date no known studies have been conducted to determine the depositional relationship between the bioherm and the clastic sediments. In order to understand this relationship and the changes this relationship caused to the environment, lateral and vertical contact relationships between the carbonate and clastic rocks must be investigated.

Early reconnaissance of the area showed the possibility of paleo-channels bisecting the bioherm. These are expressed by troughs occurring near the top of the massive bioherm, overlain by bedded limestones (Fig. 3). The cause of the bedding change is one component of this investigation. Another aspect of this investigation is to determine the cause of undulating brownish-gray and light-gray color zones within the massive part of the bioherm (Fig. 3).

The methods of investigation for this study were three fold. First a detailed topographic and geologic map was prepared, using plane-table and alidade. Areal extent of the map was determined by the length of the north-south trending bioherm and by the location of distinct stratigraphic units, above and below the bioherm; the scale of the map is 1:1800. This was followed by measuring three stratigraphic sections, spaced at equal intervals along the length of the map area and construction of an east-west structural cross-section, taken through the middle of the map area. The sections illustrate the vertical and lateral relationships between carbonate and terrigenous units. Finally, insoluble residue and petrologic investigations were done to study the cause of color zones and the changes in bedding.

GEOLOGIC SETTING

The geologic setting, in which the Laborcita Formation was deposited, began in the Early Pennsylvanian. A complex Pennsylvanian sequence of marine limestones, sandstones and shales unconformably overlap Mississippian marine limestones and minor shales. The development of these relations progressed from dominantly marine carbonates to nonmarine clastics. Basin evolution culminated, during Early-Medial Wolfcampian time, with deposition of nonmarine Abo redbeds. Paleomagnetic data from the Abo Formation places the north central Sacramento Mountains at 26 degrees south latitude at the time of deposition (Strangway, 1970).

The change in geologic setting was generated by the establishment of new north-northwest trending tectonic elements, which included the Pedernal Uplift, Sacramento Shelf and Oro Grande Basin. These new elements cut obliquely across the earlier east-west trending Mississippi Basin (Kottlowski, 1963). The rearrangement of the basin trend resulted from regional normal faulting and broad open folding, along a north-northwest trend.

The focus of deformation occurred in the central northwestern part of the present Sacramento Mountains. The greatest amount of deformation occurred during Late ›nnsylvanian and Early Permian. Four hundred feet of displacement occurred along the Fresnal Canyon fault located northeast of Alamogordo during Laborcita, pre-Abo time

(Otte, 1959). The total stratigraphic separation along this fault is about 1600 feet (Otte, 1959). Associated folding paralleled the faulting, and is characterized by broad gentle synclines and sharp narrow anticlines (Pray, 1971). Deformation of Pennsylvanian and Permian strata appears to have ended first in the northern Sacramento Mountains (Pray, 1977). This is seen by the conformable contact between the Laborcita Formation and the Abo Formation. To the south the Laborcita-Abo contact is unconformable (Pray, 1977). Deformation continued into the Late Permian, with gentle folding of the Abo-Yeso contact (Pray, 1977).

Throughout this period of tectonic adjustment, sea level of the Oro Grande Basin fluctuated greatly. During the Virgilian stage the sea level has been estimated to have changed at least 20 times with minimal drops of 100 - 150 feet (30.5 - 45.7 m) (Wilson, 1967). These periodic changes in sea level are responsible in part for cyclic sedimentary sequences.

Cyclic sequences appear in the Laborcita Formation as alternating limestone, sandstone, conglomerates and shale. These are considered by Kottlowski (1963) to be nearshore deposits laid down on the western edge of the Pedernal Landmass. Time equivalent to the Laborcita Formation is the Bursum Formation in Socorro County. This unit consists predominantly of redbeds that occur interbedded with a few

STRATIGRAPHY

The term Laborcita Formation was first proposed by Otte (1959), for strata "...consisting largely of gray and red mudstones, gray limestones, sandstones, and conglomerates, between the top of the Holder Formation and the highest marine limestone underlying the main mass of the Abo beds. The base of the type section is located 700 feet southeast of the center of section 13, T 15 S, R 10 E, at the north side of Laborcita Canyon. The top of the type section is about one mile northeast of the base." At the type locality the Laborcita Formation is 480 feet (145.9 m) thick.

Four hundred and ninety feet (150.0 m) of Laborcita Formation are exposed in the study area. Lithologies represented are alternating limestones, sandstones, conglomerates, siltstones and shales.

This repetitious sequence of rocks was attributed to cyclic changes in the sea-level in the Oro Grande Basin and to changes in drainage patterns on the Pedernal Landmass by Otte (1959), Pray (1961), and Wilson (1967).

It should be noted that gypsum occurring at most stratigraphic levels is not related to primary depositional environments. Instead it is attributed to present day environmental factors. The gypsum dune field of White Sands National Park extends for approximately thirty miles (48.4 km). The northern end of this field lies fifteen miles

(24.2 km) west of the study area. During the Spring strong southwesterly winds transport gypsum dust across the Tularosa valley. This dust has been observed by the author and Dr. Dave Johnson to be deposited in the study area. Gypsum dust has also been reported to nucleate rain drops (Johnson, personal communication) causing gypsum rain. Ground water may also be a transporting agent for the gypsum. This transport could have taken place both before and after the uplift and exposure of the strata and would account for the gypsum that occurs between bedding surfaces. These processes are believed to be responsible for the abundance of caliche and interbedded gypsum within the area.

Three stratigraphic sections were measured using a Brunton Pocket Transit. They are located in the northern, central and southern sections of the study area. These are shown on Plate 2. The rock classifications of Folk (1968) and Dunham (1962) are used for clastic and carbonate rocks, respectively. In this report the term mudstone uses Dunham's definition unless otherwise stated. Wentworth's (1922) classification is used to describe grain sizes. Descriptions of sedimentary structures are based on the classification system of McKee and Weir (1959). Sequences of clastic lithologies are listed from bottom to top. It should be noted that the glauconite mentioned within this report was identified only in hand specimens as a dull green, earthy or granular mineral. It was not x-rayed and is therefore "stratigraphers" glauconite and not mineralogic glauconite.

STRATIGRAPHY OF THE NORTHERN SECTION (A-A''')

The base of this section is marked by a four foot (1.2 m) light-gray mudstone. This mudstone has even, parallel bedding divided by shale partings. The mudstone grades vertically into a wackestone containing black, irregularly-shaped chert concressions and fine quartz sand. The top of this wackestone contains pelecypods, brachiopods, and gastropods. This wackestone is overlain by a four inch (10.2 cm), black intraclastic packstone. Black, pebble-sized, rounded mudstone intraclasts and medium-grained quartz sand occur in a light-gray mudstone matrix. This is overlain by a four foot (1.2 m) oncolitic packstone. The oncolites average two inches (5.1 cm) in diameter. Nuclei of the oncolites consist of brachiopod, gastropod, and pelecypod fragments.

Overlying the oncolitic packstone is seventeen feet (5.2m) of brown conglomerate. The conglomerate contains well-rounded, elongate, pebble to cobble-sized quartzite and rhyolite porphyry clasts. Minor amounts of chert, goethite, and mudstone are also present. Clasts are grain-supported at the base and become matrix-supported upward. The matrix is moderately sorted, medium-grained arkose and becomes poorly-sorted toward the top. Glauconite is present in the upper half of this unit. Poorly developed, low-angle, medium-scale, trough-shaped cross-stratification occurs along with even parallel bedding.

This conglomerate is overlain by twenty feet (7.6 m) of green to red, moderately sorted, medium-grained, glauconitic arkose. This arkose is calcareous and locally contains conglomerate lenses. Low-angle, medium-scale, wedge and trough-shaped cross-stratification is present.

Thirty feet (9.1 m) of red calcareous siltstone overlies this arkose. In the upper ten feet the siltstone grades into a well-sorted, fine-grained, calcareous arkose.

This arkose is overlain by two feet (0.6 m) of gray mudstone. The base of the mudstone has wavy, parallel beds marked by shale partings. This mudstone grades upward into a sandy wackestone. Medium-sized quartz, K-feldspar and lithic rhyolite porphyry grains compose the sand fraction. Ostracods are present. Rounded, symmetrical ripple laminations occur in the mudstone with 1.5 to 2 inch (3.8 - 5.6 cm) wavelengths and 0.5 inch (1.3 cm) amplitudes.

Overlying the sandy wackestone is a twenty-two foot (6.6 m) red, well-sorted, fine to medium-grained homogeneous arkose. This grades vertically into fifteen feet (4.6 m) of red, calcareous siltstone. The siltstone has discontinuous, wavy, parallel laminations.

This siltstone is overlain by a six foot (1.8 m), reddish-gray mudstone. The lower three feet (0.9 m) of mudstone are silty and contain shale partings. The top is homogeneous.

Seventeen feet (5.2 m) of red calcareous siltstone overlie this mudstone. The siltstone has discontinuous, wavy, parallel laminations. In the upper five feet (1.5 m) the siltstone grades vertically into a gray noncarbonate mudstone.

This noncarbonate mudstone is overlain by five feet (1.5 m) of greenish-gray, well-sorted, fine to medium-grained, homogeneous subarkose. This grades upward into a gray noncarbonate mudstone. Minor amounts of fissile laminations occur in the mudstone.

Overlying the noncarbonate mudstone is seven feet (2.1 m) of gray mudstone. This mudstone becomes silty upward and grades into a calcareous siltstone with discontinuous, wavy, parallel laminations.

A one foot (0.3 m) mudstone overlies this siltstone. The mudstone grades into five feet (1.5 m) of packstone, which contains black material with horizontal and domal "stromatolitic like" laminations. The black material also forms pebble-sized balls, some with visible concentric laminations. The presence of laminations suggests a blue-green algal origin for the black material, but the predominant random arrangement makes its origin problematic. Unabraded pelecypod and brachiopod shells are present in the packstone.

Overlying this packstone is fifty-seven feet (17.3 m) of green, very well-sorted, fine-grained, glauconitic, calcareous subarkose. North-east dipping, low-angle, medium-scale, wedge-shaped cross-laminations are present. Plant fossils and iron concretions occur in this subarkose. East of the measured section at the head of the northernmost canyon, the subarkose is divided by fifteen feet (4.6 m) of shale, containing iron concretions. This shale interfingers with even parallel subarkose beds along the sides of the canyon. Eastward dipping, medium-scale, high-angle, wedge-shaped cross-laminations occur in the subarkose overlying the shale (Fig. 4).

The arkose is overlain by ten feet (3.0 m) of wackestones and packstones. At the base is a two foot (0.6 m) sandy wackestone. Vertically, the wackestone grades into a ten inch (25.6 cm) intraclastic packstone. The intraclasts are pebble-sized and angular mudstone fragments. Overlying the intraclastic packstone is a five foot (1.5 m) wackestone, that contains ooids and singular, fine-grained crinoid columnals. This wackestone grades vertically into another three feet (0.9 m) of intraclastic packstone, similar to the lower packstone. This unit is ledge forming.

Overlying the intraclastic packstone is seventeen feet (5.2 m) of subarkoses, algal wackestone and siltstone. The lower eleven feet (3.3 m) of this unit is composed of green, well-sorted, fine-grained, even, parallel laminated,

Fig. 4. Photo of light-green subarkose overlying shale, arrow shows eastward dipping wedge-shaped cross-bedding.

glauconitic subarkose. The subarkose coarsens vertically and is overlain by a one foot (0.3 m) algal wackestone containing horizontally laminated stromatolites. Overlying the algal wackestone is a two foot (0.6 m) brown fissile siltstone. This siltstone grades vertically into two feet (0.6 m) of well-sorted, medium-grained subarkose. Even, parallel laminations are present in the subarkose.

Two feet (0.6 m) of gray sandy wackestone overlies the subarkose. The wackestone has sandy ripple cross-laminations and scour and fill structures. This wackestone grades vertically into eleven feet (3.3 m) of fossiliferous intraclastic packstone. Phylloid algae, bryozoans, pelecypods, and brachiopods make up the biota. Shelter pores within the packstone are filled with both white and black blocky spar. The packstone thins and pinches out to the north and east. This marks the northern end of the bioherm.

The packstone is overlain by sixty-five feet (19.8 m) of shale and interbedded packstone. The shale contains brachiopods and pelecypods. Toward the top of the shale, thin fossiliferous packstone beds are present. The biota of the packstone includes pelecypods, gastropods, brachiopods, and phylloid algae.

Overlying the shale is a seven foot (2.1 m), greenish-gray, well-sorted, medium-grained subarkose. This subarkose contains high-angle, medium-scale trough-shaped cross-laminations. Six feet (1.8 m) of dark-green, moderately-sorted, medium-grained, glauconitic arkose overlie this subarkose. This arkose is homogeneous with poorly developed, even, parallel bedding.

Six feet (1.8 m) of dark green, well-sorted, medium-grained, glauconitic arkose overlies this subarkose. The arkose is homogeneous with poorly developed, even, parallel bedding.

Overlying this arkose is a one foot (0.3 m) brownish-gray, sandy, fossiliferous wackestone. This wackestone contains medium quartz sand, as well as pelecypod and gastropod fragments.

This wackestone is overlain by seventeen feet (5.2 m) of dark-green, well-sorted, medium-grained, glauconitic arkose. This arkose is homogeneous with minor amounts of even, parallel bedding.

Five feet (1.5 m) of red siltstone overlie the arkose. Discontinuous, wavy, parallel bedding occurs in the siltstone.

This siltstone is overlain by three feet (0.9 m) of white, sandy, fossiliferous grainstone. Medium to coarse-sand grains of quartz, and pelecypod and gastropod fragments are present in the grainstone. Chert pebbles are also present. This grainstone is homogeneous.

Overlying this grainstone is five feet (1.5 m) of red siltstone. The siltstone is homogeneous and contains abundant burrows. Vertically the siltstone grades into ten feet (3.0 m) of green, moderately sorted, medium to coarse-grained, homogeneous, glauconitic, calcareous subarkose.

This subarkose is overlain by two feet (0.6 m) of white, sandy grainstone. This grainstone is homogeneous and contains medium quartz sand.

Overlying this sandy grainstone is five feet (1.5 m) of red siltstone. Discontinuous, wavy, parallel laminations are present in the siltstone.

This siltstone is overlain by a three foot (0.9 m) light-gray, moderately to poorly sorted, medium-grained, fossiliferous subarkose. The biota consists of partially abraded pelecypods and gastropods. Chert pebbles are also present. This subarkose thins abruptly to one foot to the east.

Twenty-five feet (7.6 m) of red, moderately-sorted, medium-grained arkose overlies this subarkose. The arkose is homogeneous and grades vertically into red siltstone. Discontinuous, wavy, parallel laminations occur in the siltstone.

This siltstone is overlain by a two foot (0.6 m) mudstone. Bivalve fragments are present within the mudstone. The top of this mudstone is covered by a one foot (0.3 m) sponge buildup. The sponge occurs as discrete digitate bodies in growth position. Light-gray micrite fills the intraparticle space.

Overlying the sponge buildup is fifty-nine feet (17.9 m) of siltstone, arkose, and sandy wackestone. The lower eleven feet (3.3 m) of this unit consist of red siltstone. This grades into forty-eight feet (14.6 m) of a moderately sorted, medium to coarse-grained, calcareous arkose. The arkose is homogeneous and locally has medium-scale, low-angle trough-shaped cross-laminations and lenses of matrix-supported conglomerates. Twenty-two feet (6.7 m) from the base, this arkose is divided by a one foot (0.3 m) sandy wackestone.

This arkose is overlain by a fourteen foot (4.3 m) sequence of dark-gray stromatolitic wackestone, light-gray algal packstone and fossiliferous wackestone. At the base of this sequence is one foot (0.3 m) of stromatolitic wackestone. Wavy, parallel blue-green algal laminations occur. This is overlain by ten feet (3.0 m) of homogeneous algal packstone. Gastropods are present toward the top of the packstone. The packstone grades vertically into three feet (0.9 m) of fossiliferous wackestone. Whole pelecypod and gastropod shells are present, along with crinoid columnals. Four inch (10.2 cm), irregularly shaped dissolution vugs filled with white blocky spar occur in the wackestone. This wackestone marks the uppermost unit of the Laborcita Formation in the study area.

Disconformably overlying the fossiliferous wackestone is nine feet (2.7 m) of conglomerate. This is composed of matrix-supported, cobble-sized quartzite, rhyolitic porphyry, red sandstone, and limestone clasts. Otte (1959) dated this conglomerate as Quaternary. This conglomerate caps the ridge and marks the top of the northern stratigraphic section.

STRATIGRAPHY OF THE CENTRAL SECTION (B-B''')

The base of this section is marked by a two foot (0.6 m), gray mudstone. The mudstone has even, parallel laminations. This grades upward into seven feet (2.1 m) of sandy wackestone. The wackestone contains medium to coarse-grained sand and becomes fossiliferous vertically. The biota includes pelecypods, brachiopods and gastropods. Overlying the wackestone is one foot (0.3 m) of black, intraclastic packstone containing very coarse-grained black intraclasts and medium to coarse-grained quartz. Two feet (0.6 m) of oncolitic packstone overlies the intraclastic packstone. The oncolites average two inches (5.1 cm) in diameter and have pelecypod, brachiopod and gastropod fragment nuclei.

Overlying the oncolitic packstone is a four foot (1.2 m), brown, grain-supported conglomerate. The conglomerate is composed of well-rounded, pebble-sized quartzite and rhyolite porphyry clasts with minor amounts of angular, equant mudstone. The matrix is a moderately sorted, medium-grained, calcareous arkose. Vertically the conglomerate grades into eleven feet (3.3 m) of brown arkose of the same description as the conglomerate matrix. Plant fragments are present within the arkose. The arkose is homogeneous and becomes well-sorted and glauconitic upward.

This brown arkose is overlain by twenty-five feet (7.6 m) of red, well-sorted, medium-grained, glauconitic arkose. T arkose is calcareous and is homogeneous. It becomes evenly parallel bedded upward. The top four feet (1.2 m) of the arkose becomes very well-sorted. Plant fragments and whole pelecypods occur in this arkose.

Five feet (1.5 m) of red siltstone overlies this arkose. The siltstone has discontinuous, wavy, parallel laminations.

The siltstone is overlain by a three foot (0.9 m), gray mudstone. This mudstone is silty at the base and contains wavy, parallel shale partings. The mudstone grades upward into a sandy, fossiliferous wackestone. Vertical burrows are present and filled with medium-sand. Ostracods occur within the wackestone and are concentrated in small depressions along its upper surface.

Overlying the wackestone is twenty-five feet (7.6 m) of red, moderately to poorly sorted, medium to coarse-grained, calcareous arkose. This arkose is homogeneous but has even, parallel bedding near the top.

This arkose is overlain by five feet (1.5 m) of red, calcareous siltstone. The siltstone has discontinuous, wavy, parallel laminations. This grades into one foot (0.3 m) of moderately sorted, medium-grained arkose. The arkose grades vertically back into five feet (1.5 m) of calcareous siltstone.

Two feet (0.6 m) of reddish-gray mudstone overlies the siltstone. The mudstone contains pelecypod fragments. Rounded symmetrical ripple cross-laminations are present, with a wavelength of three inches (7.7 cm) and a 0.25 inch (0.6 cm) amplitude. Silt filled vertical burrows occur at the top of this mudstone.

Overlying the laminated mudstone is twenty-eight feet (8.5 m) of red, well-sorted, medium-grained calcareous and glauconitic arkose. It is homogeneous and locally displays even, parallel bedding. Within the middle ten feet (3.0 m), this arkose grades vertically into a calcareous siltstone and then back to an arkose.

This arkose is overlain by a two foot (0.6 m), gray, silty wackestone. The base of this wackestone has even, parallel laminations. Wavy, parallel shale partings occur upward. This wackestone contains ostracods and becomes sandy at the top.

Nine feet (2.7 m) of red, well-sorted, fine-grained arkose overlie this wackestone. This contains even, wavy, parallel bedding.

This arkose is overlain by two feet (0.6 m) of gray, medium-bedded mudstone. This grades vertically into a two foot (0.6 m), variegated, packstone, containing problematic material composed of black, wavy, parallel and concentric laminations, and structureless bodies. These occur in a light-gray mudstone matrix. This grades into a three foot (0.9 m), intraclastic packstone. The top of this packstone contains whole ostracods and fragmented mollusks.

Overlying the fossiliferous wackestone is forty-nine (14.9 m) feet of light-green, well-sorted, fine-grained, glauconitic subarkose. The subarkose is calcareous and becomes medium-grained upward. Westward dipping, low-angle, medium-scale, wedge-shaped cross-laminations are present (Fig. 5). Plant fragments and iron concretions occur in the subarkose.

This subarkose is overlain by a one foot (0.3 m), coarse-grained oolitic packstone. This packstone is homogeneous and pinches out laterally to the north, south, and east.

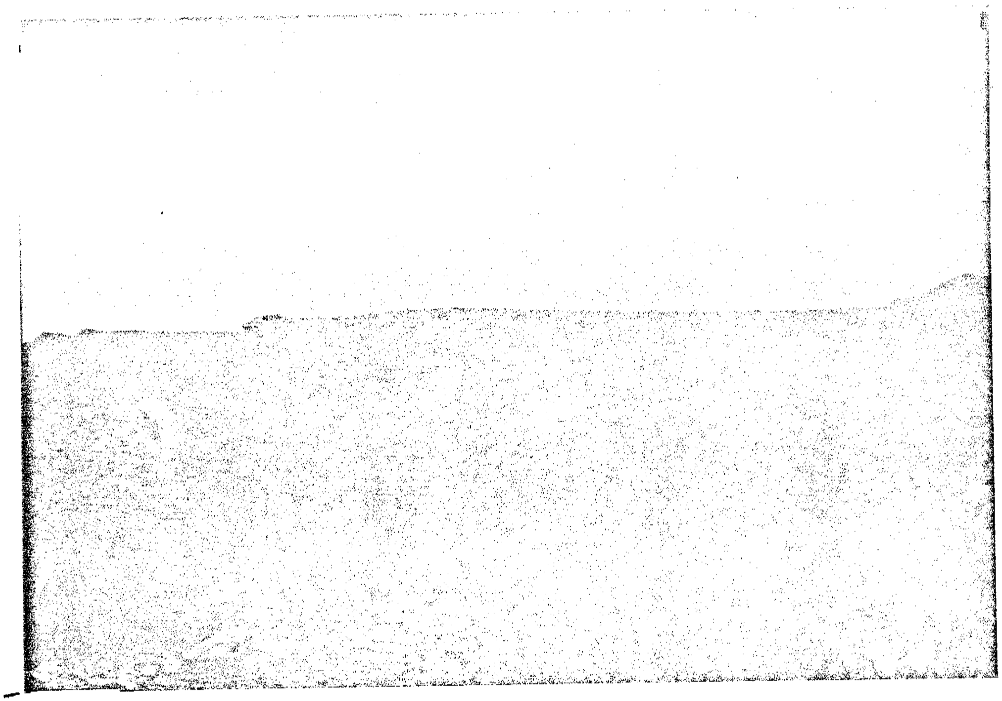

Fig. 5. Photo of westward dipping wedge-shaped cross-bedding within subarkose (arrow).

Three feet (0.9 m) of light-green, very well-sorted, fine-grained subarkose overlies this packstone. This arkose is glauconitic and calcareous. It contains westward dipping, low-angle, medium-scale, wedge-shaped cross-laminations.

This sequence of subarkose, oolitic packstone, and arkose is divided by fifteen feet (4.6 m) of shale east of the measured section along the canyon in the central part of the study area. The shale contains iron concretions and pinches out to the east and west.

The upper subarkose of this is overlain by a two foot (0.6 m), gray wackestone. The base of the wackestone is sandy and grades upward into six inches (15.2 cm) of intraclastic packstone. The intraclasts are pebble-sized, angular mudstone fragments. The packstone grades vertically into five feet (1.5 m) of light- gray, oolitic wackestone. Red, medium-grained, singular crinoid columnals are also present within the wackestone. This wackestone grades vertically back into an intraclastic packstone similar to the underlying one.

Overlying the packstone is an eleven foot (3.3 m), red, very well-sorted, fine-grained subarkose. Vertically, this grades into a medium to coarse-grained, well-sorted subarkose. A one foot (0.3 m), black, sponge packstone overlies this subarkose. The sponges are not in growth position. Overlying the packstone is six feet (1.8 m) of ght-brown siltstone. This siltstone grades vertically into green, well-sorted, medium-grained subarkose. Even, parallel bedding and laminations are present in the subarkoses and siltstone, respectively.

Two feet (0.6 m) of sandy wackestone overlies this subarkose. The top of the wackestone contains wavy, parallel stromatolitic laminations.

This is overlain by twenty-five feet (7.6 m) of thick bedded, fossiliferous, intraclastic packstone. This packstone thins and pinches out eastward, forming a mound. The biota represented are phylloid algae, bryozoans, forams, pelecypods, brachiopods, gastropods, and crinoids. Abundant shelter pores are present and filled with both black and white blocky spar. The color of the packstone grades vertically from brownish-gray to light-gray. The color abruptly returns to brownish-gray along an undulatory contact. This color change is repeated three times.

The highest homogeneous undulatory surface is overlain by a one foot (0.3 m) bed of black, fossiliferous packstone. This black packstone drapes the undulatory surface. Bryozoa, pelecypod and brachiopod fragments and whole forams are observed in the packstone. This packstone thins westward and contains intraclasts and chert pebbles. Wavy, parallel beds of light-gray packstone overlie the undulatory black packstone. These packstone beds become even vertically. A vertical sequence of facies changes occurs in t' packstone. The lower facies of this sequence is a seven foot (2.1 m), phylloid algal packstone. This packstone contains only minor amounts of precipitated spar and is overlain by a one foot (0.3 m), intraclastic, foraminiferal packstone. Overlying this is a three foot (0.9 m), fossiliferous packstone containing pelecypod, gastropod, and brachiopod shell fragments. A two foot (0.6 m), crinoidal packstone marks the top of this sequence.

Onlapping the eastern side of the carbonate mound (Fig. 6) are fifty-three feet (16.1 m) of shale, interbedded with thin, fossiliferous packstone beds. Brachiopods and pelecypods are present within the shale. The biota c tained within the packstone are pelecypods, gastropods, brachiopods and phylloid algae. The number of packstone beds varies laterally from four to six.

This shale and interbedded packstone are overlain by a six foot (1.8 m), greenish-gray, moderately sorted, medium to coarse-grained, glauconitic subarkose. The degree of sorting increases upward and grain size decreases. Medium-scale, low-angle, trough-shaped cross-laminations are present. This subarkose grades vertically into a two foot (0.6 m) siltstone. The subarkose onlaps and pinches out on the eastern side of the carbonate mound but the overlying siltstone does not pinch out.

Fig. 6. Photo of shale and overlying strata onlapping the backside of carbonate mound (arrow).

Overlying the siltstone is a one foot (0.3 m), brownish-gray, silty, fossiliferous wackestone. The biota consists of whole forams and pelecypod fragments.

Five feet (1.5 m) of greenish-gray, very well-sorted, fine-grained, calcareous subarkose overlies the wackestone. The subarkose has poorly developed, even, parallel laminations.

Overlying this subarkose is a two foot (0.6 m), reddish-gray, fossiliferous wackestone. forams, pelecypods and brachiopods represent the biota. The latter two are both whole and fragmented. The top of this wackestone becomes sandy.

This wackestone is overlain by seventeen feet (5.2 m) of greenish-gray, moderately sorted, medium-grained, glauconitic subarkose. The grain size fines upward into a fine to medium sand and then grades vertically back into coarse sand. This subarkose is homogeneous to evenly laminated.

A two foot (0.6 m), light-gray, sandy, fossiliferous wackestone overlies this subarkose. Whole forams, pelecypod and crinoid columnal fragments make-up the fossil content. The top of this wackestone reddens and contains abundant burrows.

This wackestone is overlain by twelve feet (3.6 m) of green, well-sorted, coarse-grained, glauconitic subarkose. This grades vertically into three feet (0.9 m) of red siltstone.

Overlying this siltstone is a two foot (0.6 m), sandy wackestone. This has wavy, parallel shale partings and grades into one foot (0.3 m) of sandy, fossiliferous packstone. The packstone contains pelecypod fragments.

This is overlain by seven feet (2.1 m) of red siltstone. Discontinuous, wavy, parallel laminations occur in this siltstone.

A six foot (1.8m), light-red, very well-sorted, fine-grained subarkose overlies this siltstone. This subarkose has even to wavy, parallel bedding and contains rounded, symmetrical ripple marks (Fig. 7). These ripple marks have a wavelength of five inches (12.8 cm) and amplitude of 0.75 inch (1.9 cm). Vertically, the grain size increases to coarse-sand, and sorting decreases to poorly sorted. Whole pelecypod and gastropod shells are present at the top of this subarkose along with chert pebbles. The color also changes upward to light-gray.

This fossiliferous subarkose is overlain by twenty-eight feet (8.5 m) of reddish-gray, well-sorted, medium-grained subarkose. Glauconite is present within this subarkose. The base of this subarkose contains burrows.

Fig. 7. Photo of rounded symmetrical ripple marks.

rtically, the subarkose becomes fine-grained and very well-sorted.

Overlying this subarkose is a two foot (0.6 m), gray mudstone. The top of this mudstone is covered by a one foot (0.3 m) sponge buildup. This buildup is composed of black, digitate sponges in a light-gray mudstone matrix.

Fifteen feet (4.5 m)of red siltstone overlies the sponge buildup. The siltstone grades into twenty-five feet (7.6 m) of moderately sorted, medium-grained, calcareous arkose. A two foot (0.6m) sandy, fossiliferous wackestone divides the arkose three feet (0.9 m) from the top. This wackestone contains pelecypod and bryozoan fragments. The arkose grades back into eight feet (2.4 m) of calcareous siltstone and then into five feet (1.5 m) of moderately sorted, medium-grained, calcareous arkose. The arkoses have even, parallel bedding while the siltstone contains discontinuous, wavy, parallel laminations.

Overlying this calcareous arkose is one foot (0.3 m) of dark-gray, stromatolitic wackestone. This has wavy, parallel, blue-green algal laminations and is overlain by eleven feet (3.3 m) of light-gray, phylloid algal packstone. Only minor amounts of blocky spar fill shelter pores. This packstone is overlain by three feet (0.9 m) of light-gray, fossiliferous wackestone. The biota is represented by whole shell gastropods, pelecypods, crinoids, and forams. Two to five inch (5.7 - 12.8 cm), irregular shaped dissolution vugs filled with blocky spar occur within the wackestone. This represents the uppermost unit of the Laborcita Formation in the study area.

Unconformably overlying this wackestone are eight feet (2.4 m) of Quaternary conglomerate (Otte, 1959). This contains cobble-size quartzite, rhyolite porphyry, red sandstone, and limestone clasts in an arkosic matrix. This conglomerate caps the ridge and marks the top of the central section.

STRATIGRAPHY OF THE SOUTHERN SECTION (C-C''')

The base of the southern section is marked by a six foot (1.8 m), light-gray mudstone. The mudstone contains trace amounts of medium-grained quartz sand. This grades vertically into a sandy, fossiliferous wackestone. Pelecypods, gastropods, brachiopods, rugose coral, and sponges occur in the wackestone. This is overlain by eight inches (20.5 cm) of black, mudstone intraclastic packstone. Black, pebble-sized, rounded intraclasts and medium-grained quartz sand are present in a light-gray mudstone matrix. Overlying the packstone is a four foot (1.2 m), oncolitic packstone. The oncolites average two inches (5.1 cm) in diameter (Fig. 8). Pelecypod, gastropod and brachiopod fragments form the nuclei of the oncolites.

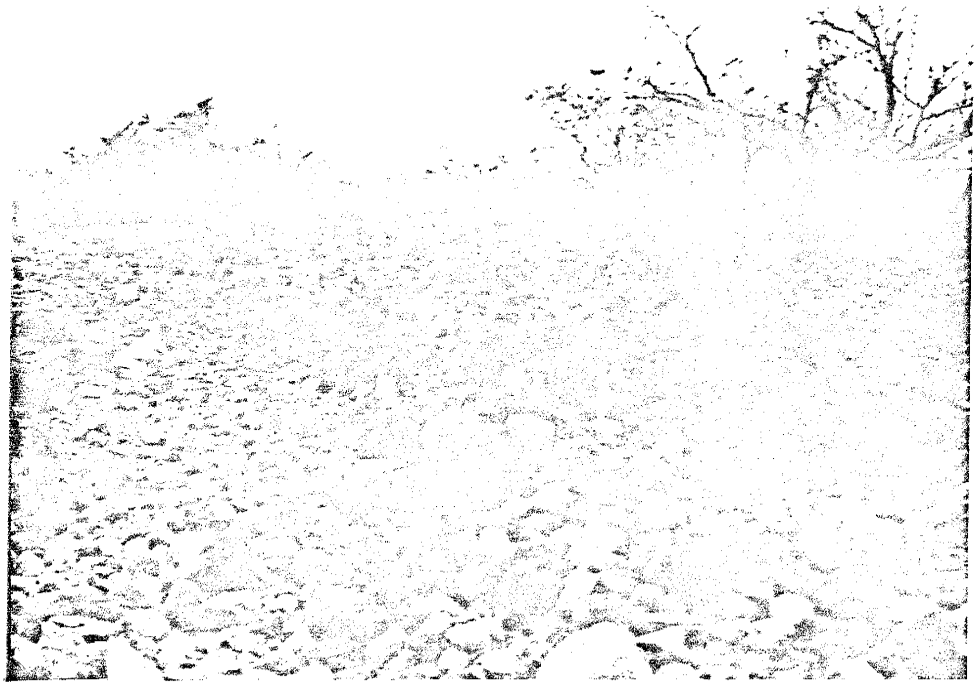

Fig. 8. Photo of oncolitic lag.

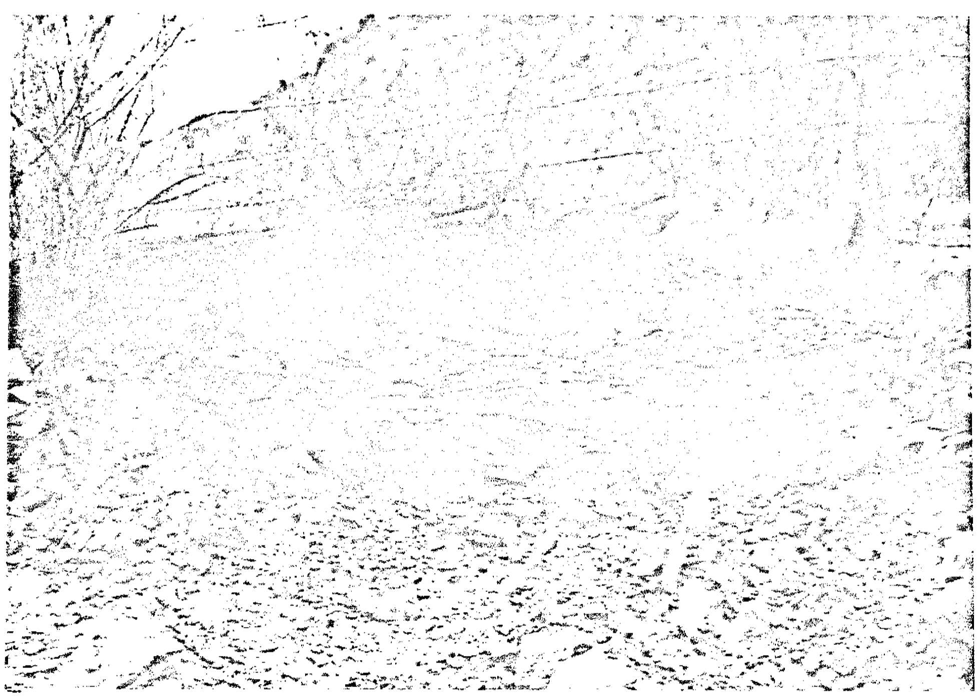

Fig. 9. Photo of trough-shaped cross-stratified arkose.

Overlying the oncolitic packstone is twenty-two feet (6.7 m) of light-brown, well-sorted, medium-grained arkose. The grain size increases vertically to coarse-sand. This is accompanied by a decrease in sorting to poorly sorted. Locally, cobble-sized quartzite and rhyolite porphyry clasts are present. Fossilized wood is also found within the arkose. The upper six feet (1.8 m) of this arkose becomes well-sorted and fine-grained. The well-sorted portion of the arkose is homogeneous while the poorly sorted arkose has low-angle, medium-scale, trough-shaped cross-laminations (Fig. 9). The upper half of this arkose is glauconitic.

This arkose is overlain by four feet (1.2 m) of red and green, calcareous siltstone with discontinuous, wavy, parallel laminations.

This siltstone is overlain by a one foot (0.3 m), gray mudstone. The base of the mudstone has wavy, parallel shale partings and even, parallel bedding occurs near the top. The mudstone grades into a two foot (0.6 m), fossiliferous wackestone. The wackestone contains ostracods and phylloid algae. The ostracods are concentrated along thin, even, parallel bedding surfaces.

Overlying the fossiliferous wackestone is a five foot (1.5 m), reddish-brown, grain-supported conglomerate. It is composed of very well-rounded, elongate, cobble-sized quartzite, rhyolite porphyry, chert, and angular mudstone clasts in a well-sorted, medium-grained, arkosic matrix.

The clasts are randomly oriented. Glauconite grains and micrite cement are present within the matrix. The base of the conglomerate shows little signs of erosion.

The conglomerate is overlain by thirty-two feet (10.6 m) of green, well-sorted, medium to coarse-grained, glauconitic arkose. The grain size of the arkose alternates vertically between medium and coarse-sand grading to fine-sand at the top. Poorly developed, low-angle, medium-scale, trough-shaped cross-laminations occur within the coarser grained arkose while even, parallel laminations are present in the finer-grained arkose.

Overlying this arkose is ten feet (3.0 m) of red, calcareous siltstone. The siltstone has discontinuous, wavy, parallel laminations, and locally contains mudstone lenses. A two foot (0.6 m), green, moderately sorted, medium-grained, glauconitic arkose lens divides the siltstone. The arkose is homogeneous.

This siltstone is overlain by a four foot (1.2 m), reddish-brown conglomerate (Fig. 10). The conglomerate is grain-supported and contains well-rounded, elongate, randomly oriented quartzite, rhyolite porphyry and chert cobbles along with angular mudstone cobbles. The matrix is composed of poorly sorted, medium-grained, glauconitic, calcareous arkose. The thickness of this conglomerate varies laterally from two to six feet (0.6 - 1.8 m). Little evidence of erosion is observed along the base of the conglomerate.

Eleven feet (3.3 m) of red, calcareous siltstone overlies the conglomerate. The siltstone has discontinuous, wavy, parallel laminations.

This siltstone is overlain by a twenty-one foot (6.4 m), gray, sandy wackestone. The wackestone contains medium quartz sand and has wavy, parallel shale partings. It grades vertically into a one foot (0.3 m) mudstone and interfingers with the underlying siltstone. The top of the mudstone contains fissile laminations and ostracods.

Overlying the mudstone is ten feet (3.0 m) of light-brown to green, moderately to poorly sorted, coarse-grained, glauconitic arkose. Vertically, it grades to a well-sorted, fine to medium-grained arkose. This arkose is calcareous and homogeneous.

A seven foot (2.1 m), gray mudstone overlies this arkose. The base of this mudstone has even, parallel laminations. These grade vertically to even, parallel beds and then back to even, parallel laminations at the top. The beds are defined by shale partings.

This mudstone is overlain by six feet (1.8 m) of variegated light and dark-gray packstone. Within the black packstone local wavy, parallel laminations and pebble-sized, concentrically layered balls occur. This suggests the possibility of their being blue-green algae. This black

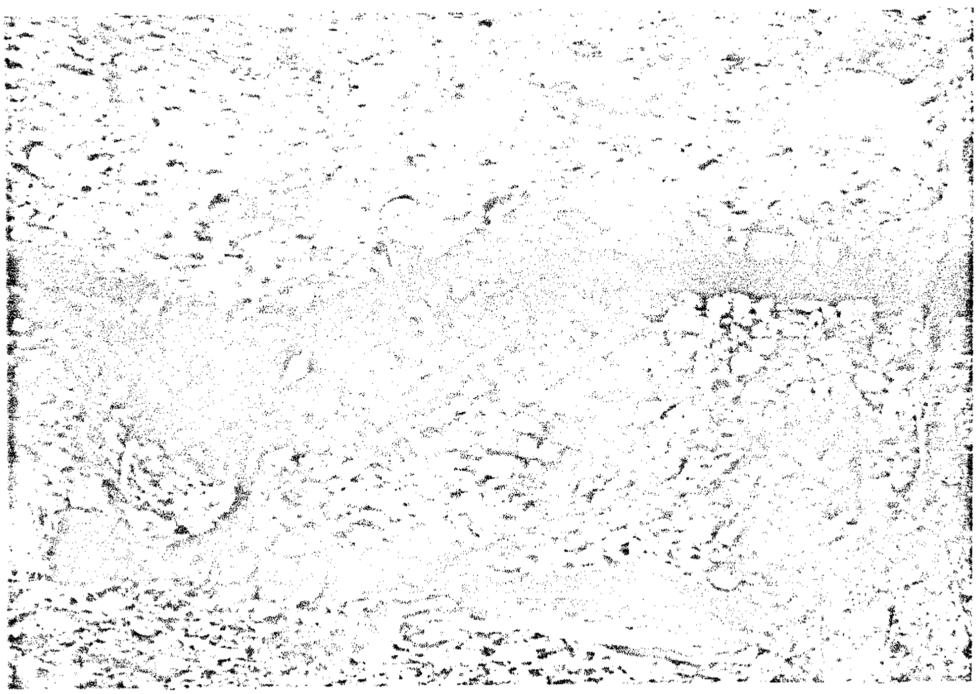

Fig. 10. Photo of brown, grain-supported, cobble conglomerate showing little erosion at the base and random orientation of clasts.

material also appears as pebble-sized, unstructured, irregularly shaped bodies. These problematica occur in a light-gray mudstone matrix. Whole shell pelecypods and brachiopods are present at the top of this packstone along with bryozoan fragments.

Overlying the packstone is a forty-six foot (14.0 m), light-gray, very well-sorted, fine to medium-grained subarkose. The subarkose has even, parallel laminations. Pelecypod fragments, fossilized wood fragments and iron concretions are present. Moving eastward from the measured section along the southernmost canyon in the study area, this subarkose is divided by fifteen feet (4.6 m) of shale. The shale contains iron concretions. It thins to the east and is interbedded with subarkose at the head of the canyon. Rounded symmetrical ripple marks with a wavelength of five inches (12.8 cm) and an amplitude of 0.75 inch (1.9 m) occur in the subarkose at the head of the canyon. These are overlain by eastward dipping, medium scale, high-angle cross-laminations. Overlying these are even, parallel beds, containing burrows.

An eight foot (2.4 m), gray wackestone-packstone overlies this subarkose. The base of this wackestone is sandy. It grades vertically into an eight inch (20.5 cm), intraclastic packstone. The intraclasts are pebble-sized and angular. The packstone grades upwards into three feet (0.9 m) of wackestone containing medium-grained ooids and single crinoid columnals. This wackestone grades vertically back into two feet (0.6 m) of intraclastic packstone.

Overlying the intraclastic packstone is eleven feet (3.3 m) of green, well-sorted, medium to coarse-grained arkose. This arkose becomes coarser vertically and is overlain by ten inches (25.6 cm) of black, fossiliferous packstone. Digitate sponge and pelecypod fragments are the only fossils present. Overlying this packstone is a six foot (1.8 m), light-brown, fissile siltstone. This grades vertically into a seventeen foot (5.2 m), green, well-sorted, medium-grained subarkose. Even, parallel beds occur in the subarkose and arkose.

A two foot (0.6 m), dark-gray wackestone overlies the subarkose. This wackestone is sandy at the base and is overlain by a thirty foot (9.4 m) fossiliferous, intraclastic packstone. Phylloid algae, brachiopods, pelecypods, bryozoans, forams and trilobites represent the fauna within the packstone. The color of the packstone grades vertically from brownish-gray to light-gray. The top of the light-gray zone is marked by a sharp return to brownish-gray. The contact between the two colors is undulatory. This change in color occurs three times along the western face of the packstone. The packstone contains abundant black and white spar in shelter pores. It thins and pinches out eastward, forming a mound.

Overlying this packstone is a sequence of wavy, parallel bedded, intraclastic packstone, phylloid algal packstone, foraminiferal wackestone, fossiliferous packstone and crinoidal packstone. The base of this sequence is marked by the presence of a one foot (0.3 m), black, intraclastic packstone. This contains pebble-sized intraclasts along with forams, bryozoan, pelecypod, and brachiopod fragments. This is overlain by four feet (1.2 m) of light-gray, phylloid algal packstone. Very little precipitated spar is present in this packstone. This grades into a one foot (0.3 m), light-gray, foraminiferal wackestone. Overlying this is three feet (0.9 m) of gray, fossiliferous packstone. The biota consists of pelecypod, brachiopod, and gastropod fragments. The gray packstone grades into a two foot (1.2 m), crinoidal packstone. The crinoids are articulate. Pelecypod, brachiopod, and gastropod fragments occur within this packstone, along with forams.

Onlapping the eastern side of the packstone is a fifty-seven foot (17.3 m), fossiliferous shale interbedded with thin, fossiliferous packstone beds (Fig. 11). Brachiopods and pelecypods are present within the shale. The biota in the packstone consists of phylloid alga, pelecypods, brachiopods, and gastropods. The number of interbedded packstones varies laterally from four to six. These packstones are most abundant near the top of this unit.

Fig. 11. Photo of shale onlapping the backside of the carbonate mound. Sierra Blanca can be seen in the background.

The interbedded shales and packstones are overlain by a seven foot (2.1 m), greenish-gray, moderately-sorted, medium to coarse-grained subarkose. The sedimentary structures present within the subarkose are medium-scale, high-angle, trough-shaped cross-laminations (Fig. 12).

Overlying this subarkose is a one foot (0.3 m), brownish-gray, fossiliferous packstone. Pelecypod and gastropod fragments are present in this packstone along with crinoid columnals. It grades into three feet (0.9 m) of fossiliferous wackestone that contains pelecypod and gastropod fragments. The wackestone grades vertically into a one foot (0.3 m), sandy, fossiliferous packstone. The same biota represented in the wackestone occurs in the packstone. The two packstones are homogeneous, while the wackestone contains wavy, parallel bedding.

Twenty feet (6.1 m) of greenish-gray, well-sorted, fine to medium-grained, glauconitic subarkose overlies the packstone. The subarkose has even bedding but is locally homogeneous.

Overlying this subarkose is a four foot (1.2 m), white, sandy, fossiliferous wackestone. The wackestone contains pelecypods and ostracods. Wavy, parallel shale partings occur in the wackestone. Burrows are present along the top of this bed.

Fig. 12. Photo of trough-shaped cross-bedded subarkose overlying shale with interbedded packstone. Diabase dike also shown cutting shale and subarkose.

This is overlain by a four foot (1.2 m), red, well-sorted, medium-grained, glauconitic subarkose. The subarkose has even, parallel bedding and grades upward into a two foot (0.6 m) siltstone. The siltstone has discontinuous, wavy, parallel laminations.

A two foot (0.6 m), gray, sandy, fossiliferous wackestone overlies this siltstone. Pelecypod fragments are present in the wackestone. The wackestone has wavy, parallel shale partings.

Overlying the wackestone is a six foot (1.8 m), red siltstone. Discontinuous, wavy, parallel laminations are present in the siltstone.

This siltstone is overlain by a six foot (1.8 m), white, well-sorted, medium-grained, subarkose. The base has even, parallel bedding and contains ripple marks. These have a wavelength of six inches (15.4 cm) and an amplitude of 0.75 inches (1.9 cm). Vertically, the subarkose becomes poorly sorted and coarse-grained. Whole pelecypod, gastropod and nautiloid shells occur at the top of this subarkose along with chert pebbles.

Eleven feet of red, well-sorted, medium-grained subarkose overlies this subarkose. Worm burrow traces are present at the base. The subarkose becomes green, fine-grained and glauconitic upwards. It is homogeneous throughout.

This subarkose is overlain by fourteen feet (4.3 m) of red siltstone. Discontinuous, wavy, parallel laminations occur in the siltstone.

Overlying the siltstone is a three foot (0.9 m), gray, homogeneous mudstone. The base of the mudstone is sandy, while the top of this mudstone is covered by a one foot (0.3 m) digitate sponge buildup. The sponges are in growth position and surrounded by light-gray mudstone matrix.

The sponge buildup is overlain by a sixteen foot (11.8 m), red siltstone with discontinuous, wavy, parallel laminations. This grades vertically into twenty-one feet (6.4 m) of moderately to poorly sorted, medium-grained arkose. Locally, quartzite and rhyolite porphyry cobbles are present. The arkose is homogeneous to poorly bedded. It grades vertically into a two foot (0.6 m), gray, sandy, fossiliferous wackestone. This wackestone contains pelecypod fragments and is homogeneous. It grades vertically into a twenty-two foot (6.7 m), red, calcareous siltstone with discontinuous, wavy, parallel laminations.

A one foot (0.3 m), dark-gray stromatolitic wackestone overlies this siltstone. The wackestone contains wavy, parallel, blue-green algal laminations. It is overlain by six feet (1.8 m) of phylloid algal packstone. This packstone is homogeneous and contains only minor amounts of precipitated spar. This packstone represents the top of the Laborcita Formation in the study area.

Unconformably overlying the packstone is a six foot (1.8 m), Quaternary grain-supported conglomerate (Otte, 1959). This conglomerate is composed of rounded quartzite, rhyolite porphyry, red arkose, and limestone cobbles in a brown arkose matrix. This conglomerate caps the hill and marks the top of the stratigraphic section in the southern section.

COLOR AND BEDDING CHANGES WITHIN THE BIOHERM

Along the exposed sides of the bioherm distinct patterns can be observed. These occur in two forms. The first form is undulating patterns seen as a vertical, gradational change in color from brownish-gray to light-gray. This is followed by a sharp return to brownish-gray (Fig. 13). The second form is a change along an undulating surface from homogeneous to wavy, parallel bedding (Fig. 14).

The change in bedding was at first believed to represent channelways connecting the shelf with lagoonal waters. It was thought that clastic sediments might have been transported through these channels in a fashion similar to the clastic paleo-channels that bisect Virgilian bioherms in the southern Sacramento Mountains (Wilson, 1967).

In order to determine the cause of these patterns, samples were collected at two locations representative of the color changes, and at three locations where bedding changes occur. Insoluble residues and petrographic analyses were done to determine whether differences in color and bedding were the result of depositional or diagenetic changes.

Fig. 13. Photo of gradational color change from brownish-gray to light-gray.

Fig. 14. Photo of thin bedded limestones draping massive limestone.

COLOR CHANGES

The color changes from brownish-gray to light-gray occur along the exposed faces of the bioherm. This change occurs three times. The undulating color changes are usually parallel to each other. An exception to this may be seen in Fig. 13. The change in color occurs across a four to eight foot (1.2 - 2.4 m) interval.

Insoluble Residue

Two locations were chosen to investigate the cause of the color change, one in the northern part of the study area and the other in the southern part. In the northern area samples were collected from four intervals: A) within the light-gray zone, one foot (0.3 m) below the contact between the light-gray and brownish-gray color change; B) within the light-gray zone one inch (2.54 cm) below the contact; C) within the brown-gray zone one inch (2.54 cm) above the contact; and D) within the brown-gray zone one foot (0.3 m) above the contact.

Sampling of the color change was more extensive in the south due to accessibility. Six samples were collected at this location: A) within the brownish-gray zone five feet (1.5 m) below the contact between the light-gray and brownish-gray coloring; B) within brownish-gray zone three feet (0.9 m) below the color contact, where it begins to grade to light-gray; C) within the light-gray zone one foot (0.3 m) below the color contact; D) within the light-gray one one inch (2.54 cm) below the color contact; E) within the brownish-gray zone one inch (2.54 cm) above the color contact; and F) within the brownish-gray zone one foot (0.3 m) above the color contact. The results of this investigation are enumerated in Fig. 15.

Statistical Analysis

In order to test the significance of the insoluble residue data, the Kruskal-Wallis H test for nonparametric statistics was used. In this test a calculated critical value (h) is compared with a tabulated chi-square variable with K-1 degrees of freedom, where K is the total number of categories compared (see Walpole and Myers, 1978 p. 496). level of significance of 0.05 is used in the two-tailed test. This test is used to check the null hypothesis that K independent samples are from identical populations, where K > 2. If the calculated h value is greater than the tabulated chi-square value, then the null hypothesis is rejected.

The following formula is used in the calculations:

$$h = \frac{12}{n(n+1)} \sum_{i=1}^{K} \frac{r_i^2}{n_i} - 3(n+1)$$

where

h = calculated critical value

n = total number of observations

n_i = total number of observations in sample i

r_i = sum of ranks corresponding to n

Fig. 15. Plots showing variations in percent insoluble residue vs. sample location for color changes. Dashed line indicates mean.

ation 1

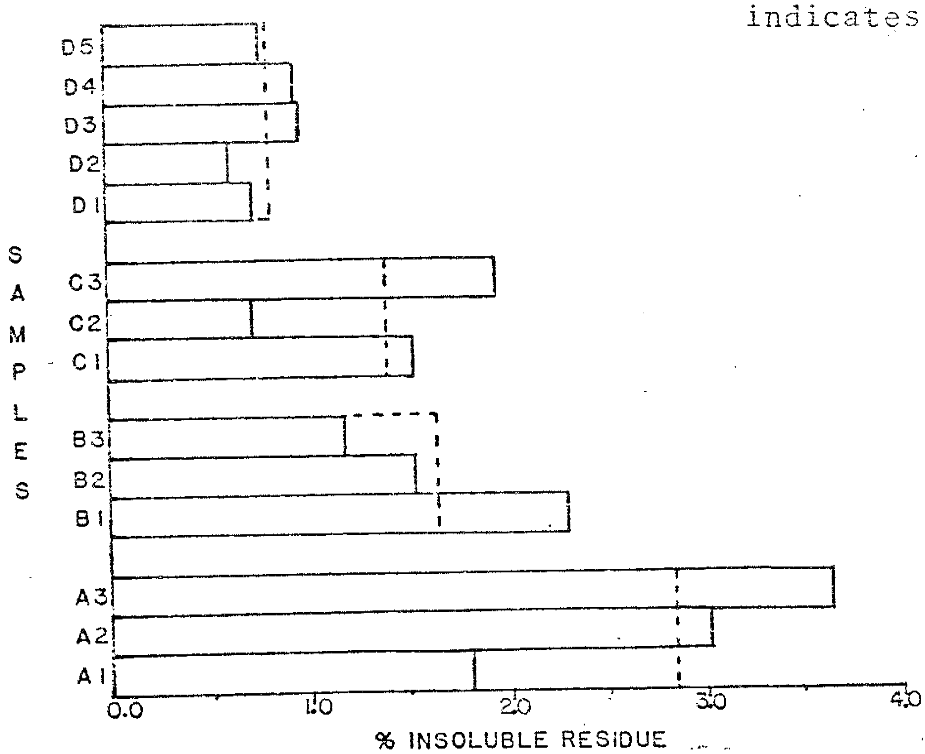

cation 2

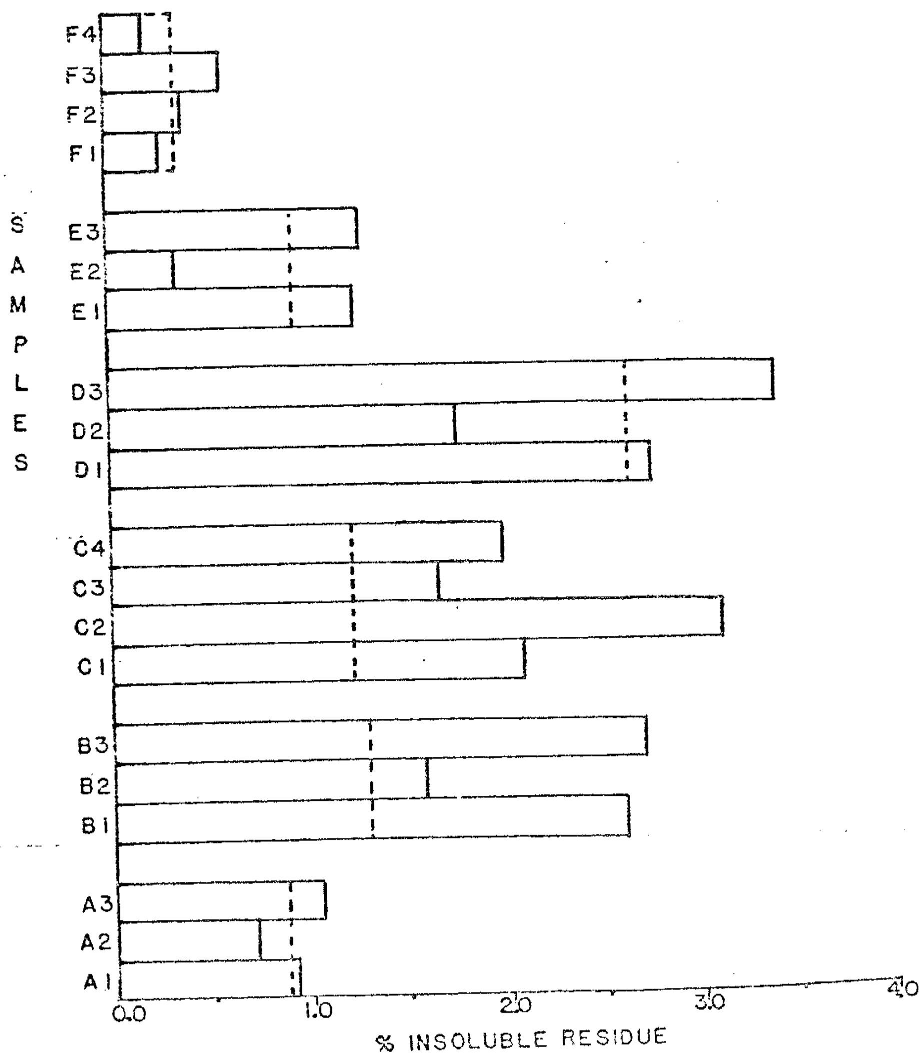

observations in the i sample.

The results of the Kruskal-Wallis H test for both the northern and southern locations accept the null hypothesis that samples from different color zones are from the same population. This means that no significant change in the amount of insoluble residue occurred within the depositional environment. The percentage of insoluble residue can be further evaluated by redefining the samples based upon color. In this case, all brownish-gray sample locations at an outcrop are combined into one sample and all light-gray sample locations are combined into another sample. To determine whether the brownish-gray samples are from another population than the light-gray samples the Wilcoxon rank-sum test is used (Walpole and Myers, 1978, p. 476). This test is similar to the Kruskal-Wallis H test, except that it is restricted to the comparison of two samples. The following formulas are used in the calculations:

$$u_1 = w_2 - \frac{n_1(n_1+1)}{2}$$

where

u_1 = critical value of the smaller sample

w_1 = the sum of the ranks in the smaller sample

n_1 = the number of observations in the smaller sample

and

$$u_2 = w_2 - \frac{n_2(n_2+1)}{2}$$

where

u_2 = critical value of the larger sample

w_2 = the sum of the ranks in the larger sample

n_2 = the number of observations in the larger sample.

When n < 8, the null hypothesis is accepted if twice the tabulated level of significance is greater than or equal to the two-tailed test level of significance, 0.05. The tabulated level of significance is based on the degrees of freedom and the size of the two samples. For tests where n > 8, the null hypothesis is accepted when the lowest critical value is greater than a tabulated critical value. The tabulated critical value is based on the values of n , n and the two-tailed test level of significance, 0.05.

The results of this test show that the null hypothesis is rejected at both locations. Therefore, there is a difference between the percent insoluble residue within the brownish-gray zone and the light-gray zones. The difference being that the light-gray zone contains more insoluble residue.

With this information, it can be concluded that individual samples taken across the transition from brownish-gray to light-gray are from the same population, i.e. the same depositional environment, as demonstrated by the Kruskal-Wallis H test. Within this depositional environment, minor changes occurred where a greater percentage of insoluble residues were deposited in the light gray zone.

PETROGRAPHIC STUDY

Six thin sections were made from samples representative of the six zones at the southern location. From these the percentage and types of intraclasts, ooids, peloids, skeletal material, micrite, neomorphic spar, precipitated spar, terrigenous debris, organic material and pore space were determined (Fig. 16) by visual estimate using the visual percentage estimation chart of Terry and Chilinger (1955), along with the sequence of diagenetic events. The term skeletal is used within this report for material derived from organisms and consisting of hard parts secreted by organisms or of the hard material around or within the organic tissue.

By comparing the percentage of various constituents, differences between the brownish-gray zones and light-gray zones can be seen. These differences occur in the amount of skeletal material, micrite, neomorphic spar and precipitated spar.

Fig. 16. Plots showing variations in percent constituents vs. color zones for study location 2.

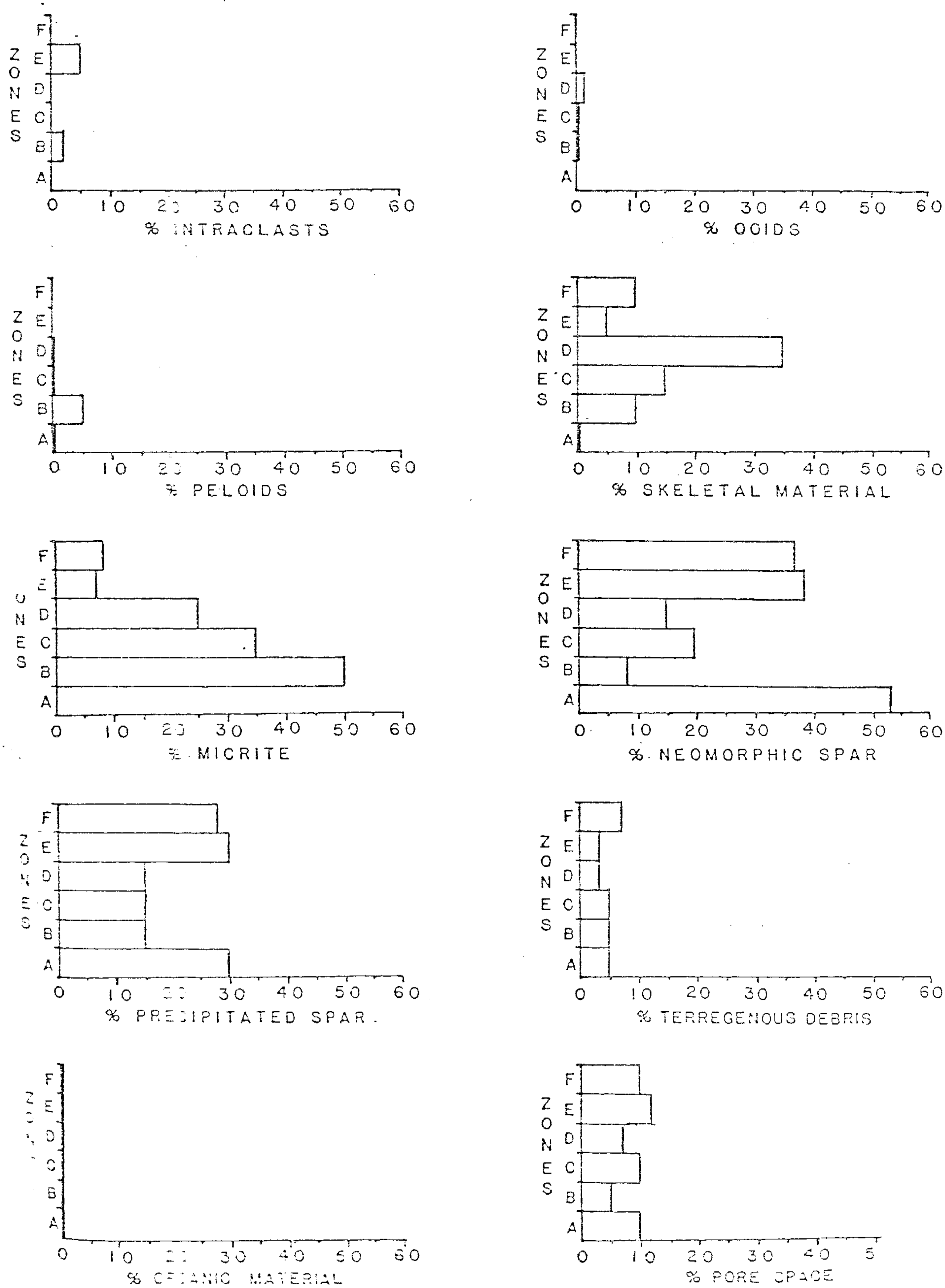

The variation of percent skeletal material is gradual. In the lowermost brownish-gray zone only trace amounts of phylloid algae and crinoid columnals can be recognized. As the color changes to light-gray the percentage increases to 10, 15 and 35 in zones B, C, and D, respectively. The types of skeletal material remain the same within these zones and include ostracods, bryozoans, phylloid algae, forams, pelecypods, gastropods, brachiopods and crinoid columnals. Above the sharp return to brownish-gray, the proportion of skeletal material decreases markedly to 5%. Phylloid algae, ostracods, bryozoans and crinoid columnals constitute the biota in this zone. In the next foot (0.3 m), the amount of skeletal material increases to 10% with only phylloid algae being recognized. Micrite envelopes are found on phylloid algae, pelecypods and gastropods. Burrows are present in all zones.

The next variation to consider is in the amount of micrite. Percentages are lowest in the brownish-gray zone. In zones A, E and F, the percentage of micrite is 2, 7 and 8, respectively. These contrast with the light-gray zones B, C and D, where 55, 35 and 25% micrite occurs, respectively.

The abundance of neomorphic spar also varies between the color zones, with the brownish-gray zone containing the greater percentage of neomorphic spar. In zones A, E and F, 53, 38 and 37% neomorphic spar occurs respectively. These compare with zones B, C and D, in the light-gray zones where the percentage of neomorphic spar is 8, 20 and 15, respectively. Within the light-gray zones, neomorphism of micrite to microspar and pseudospar is less developed than in the brownish-gray zones. Pseudospar averages 0.3 mm in diameter in zone A, 0.8 mm in zone E and 0.7 mm in diameter in zone F. The crystal contacts between the pseudospar are irregular and sutured in these zones. In the light-gray zones the size of the pseudospar crystals average 0.1 mm in diameter. The crystal contacts between the pseudospar are irregular in these zones. Microspar and pseudospar are replacing micrite matrix and phylloid algae in the light-gray zones. Ghost structures of precipitated spar are seen within the neomorphic spar.

The percentage of precipitated spar is greater in the brownish-gray zones than the light-gray zones. Precipitated spar within all light-gray zones composes 15% of the sample. This compares with the brownish-gray zones where precipitated spar accounts for 30% within zones A and E, and 28% within zone F. The types of precipitated spar that occur in both zones are drusy and blocky. They are found in burrow, moldic, shelter, dissolution and fracture pores. Within the samples studied in zones A and F, ghosts of radial fans (Toomey and Cys, 1979) occur. The width of an individual needle is .15 mm, with lengths reaching 1.5 cm. The ends of needles are square. These radial fans are found in shelter pores, coating phylloid algae and forams. Fans are also in contact with blocky spar and micrite. Another form of precipitated spar observed in zone A is syntaxial rim cement coating a crinoid columnal.

Sequence of Diagenetic Events

The sequence of diagenetic events is similar in both the brownish-gray zones and the light-gray zones. The differences occur in the degree of neomorphism. The stages of diagenesis are based on work by Longman (1980).

Following deposition, burrowing occurred and micrite envelopes formed on algal plates and bryozoans. During this time lime mud was micritized and spar precipitated within zooecia of bryozoa and other intraparticle pore space. Radial fans were precipitated at this time. The primary evidence for this is the way that growth of blocky spar appears to be restricted by the presence of radial fans. Petrographic investigation by Toomey and Cys (1979) of the same bioherm found encrusting forams and algae on the radial fans supporting the above conclusion. Longman (1980) determined that radial fibrous aragonite needles are precipitated within the active marine phreatic zone. Processes within this zone include circulation of sea water through the pores. No leaching occurs, and aragonite and/or low Mg-calcite may be precipitated. The presence of decaying organic material raises the Eh of the pore water and facilitates precipitation. It should be noted that fabric studies by Otte and Parks (1961) concluded that these fans had an organic origin and believed them to be a form of stromatactis. This conclusion is supported by a study by Bathurst (1959) of the stromatactis reefs in Lancashire, England.

The third stage of diagenesis took place in a fresh water phreatic environment. Longman (1980) divided this environment into three zones, the stagnant zone, active zone and zone of solution. Transition through all of these zones can be seen within the brownish-gray areas of the bioherm.

This transition begins in the stagnant zone, where there is little or no water movement. The water is saturated with calcium carbonate. For this reason, little if any leaching and only minor cementation occurs. Instead, neomorphism of aragonite takes place with some original textures being preserved. This can be seen by the ghost of radial fan aragonite needles in neomorphic spar (Fig. 17).

The diagenetic environment became more active. Water circulating through the pores, leached and replaced unstable grains and rapidly precipitated cement. While in this environment, the interiors of the algal blades were leached, forming moldic pores. These moldic pores and remaining shelter pores were filled with equant calcite. The crystals grew coarser as the pores were filled. Syntaxial rim cement also formed on crinoid columnals. Longman (1980) has found that these types of cement indicative of the active freshwater phreatic environment.

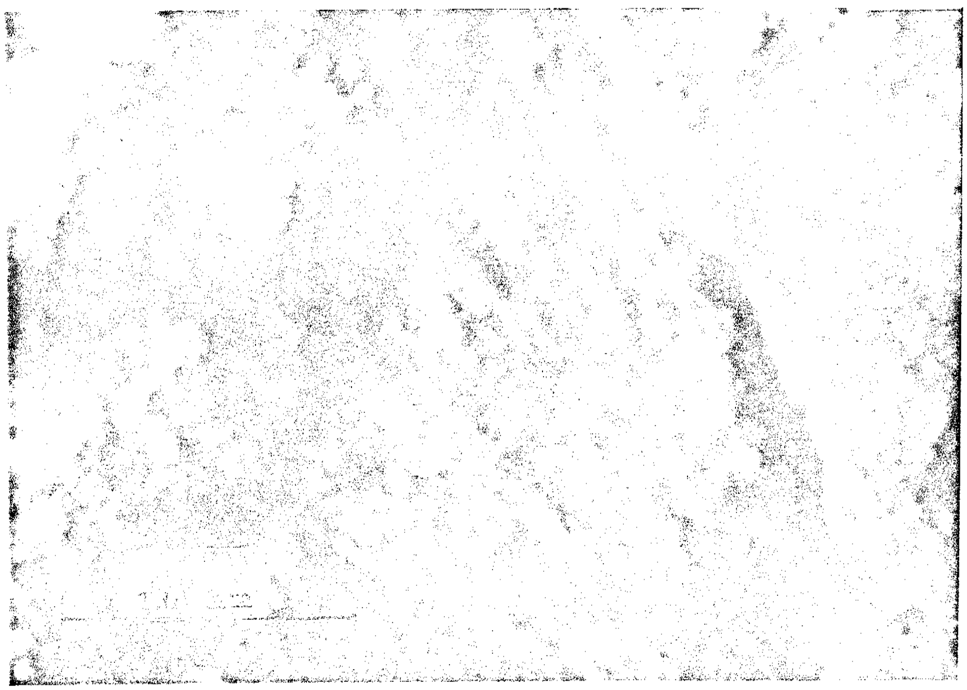

Fig. 17. Photomicrograph of neomorphosed radial fan.

The final phase of diagenesis occurred in the freshwater phreatic zone of solution. In this zone meteoric water is undersaturated in calcium carbonate. This condition causes dissolution of calcium carbonate and formation of vuggy pores.

Diagenetic changes followed the same transitions in the light-gray zone as the brownish-gray zones. The lack of shelter pores did not allow for the precipitation of radial fan aragonite while in the active marine phreatic zone. Another difference occurred while in the fresh water phreatic zone. Under these conditions the degree of neomorphism decreased.

SUMMARY

The cause for the undulatory zonation within the bioherm must be based more on the changes in initial deposition rather than on later diagenetic changes. The difference in degree of neomorphism is not wholly understood. It could possibly be due in some way to greater percentage of micrite within less neomorphosed zones. The significance of changes in depositional environment will be discussed in the following chapter.

BEDDING CHANGES

Along the top of the bioherm, the bedding changes from zoned to wavy, parallel beds. This is most noticeable where parallel beds curve downward in a trough shape (Fig. 14).

The contact between the two bedding types is marked by a one foot (0.3 m), black packstone. This packstone is continuous across the rises between the troughs. It thins toward the west and contains chert pebbles. At the outset of this investigation it was thought that these trough-shaped structures might represent paleo-channels that fed into a larger channel bisecting the bioherm at the site of the present day canyon. The lack of binding organisms within this channel would make it less resistant to weathering than the bioherm. This would allow the channel to be more readily eroded creating a canyon. The only evidence remaining of the large channel would be the tributary channels. The presence of the bedded packstone, draping both troughs and crests, discounts the possibility of these structures being tributary paleo-channels. Close examination of these troughs show them to be depressions rather than linear troughs.

Another cause for the change in bedding is therefore needed. The most likely cause would be a change in depositional environment. In order to determine the type of change, samples for insoluble residues and petrographic analysis were collected along three depressions. Two of these are located on the northern side of the central canyon, and the third on the southern side. Thin sections were made and analyzed from the most western depression on the north side of the canyon.

INSOLUBLE RESIDUE

Samples were collected from five locations across the bedding changes. These locations were: A) one foot (0.3 m) below the base of the black packstone; B) one inch (2.54 cm) below the black packstone; C) within the black packstone; D) one inch (2.54 cm) above the black packstone; and E) one foot (0.3 m) above the black packstone. The percentage of insoluble residues was determined for the sample location. The results are found in Figure 18.

Statistical Analysis

To determine if there are statistically valid differences in percentage of insoluble residue at the different sample locations, the Kruskal-Wallis H test was used. This method has been discussed previously.

At all three study locations the null hypothesis, stating that the samples all came from the same population, is rejected. Therefore, there is a difference in the percent insoluble residue at the sample locations. By comparing the mean percentage of insoluble residue from the different sample locations, a difference is seen between the two easternmost study locations and the western study location. At the eastern locations, a marked increase in the percent insoluble residue occurs within the black packstone. This increase is followed by a sharp decrease to the lowest percentage of insoluble residue at the sample location one inch above the black packstone. This trend is

Fig. 18. Plots showing variation in percent insoluble residue vs. sample locations for bedding changes at study locations 3, 4, and 5. Dashed line indicates mean.

Location 3

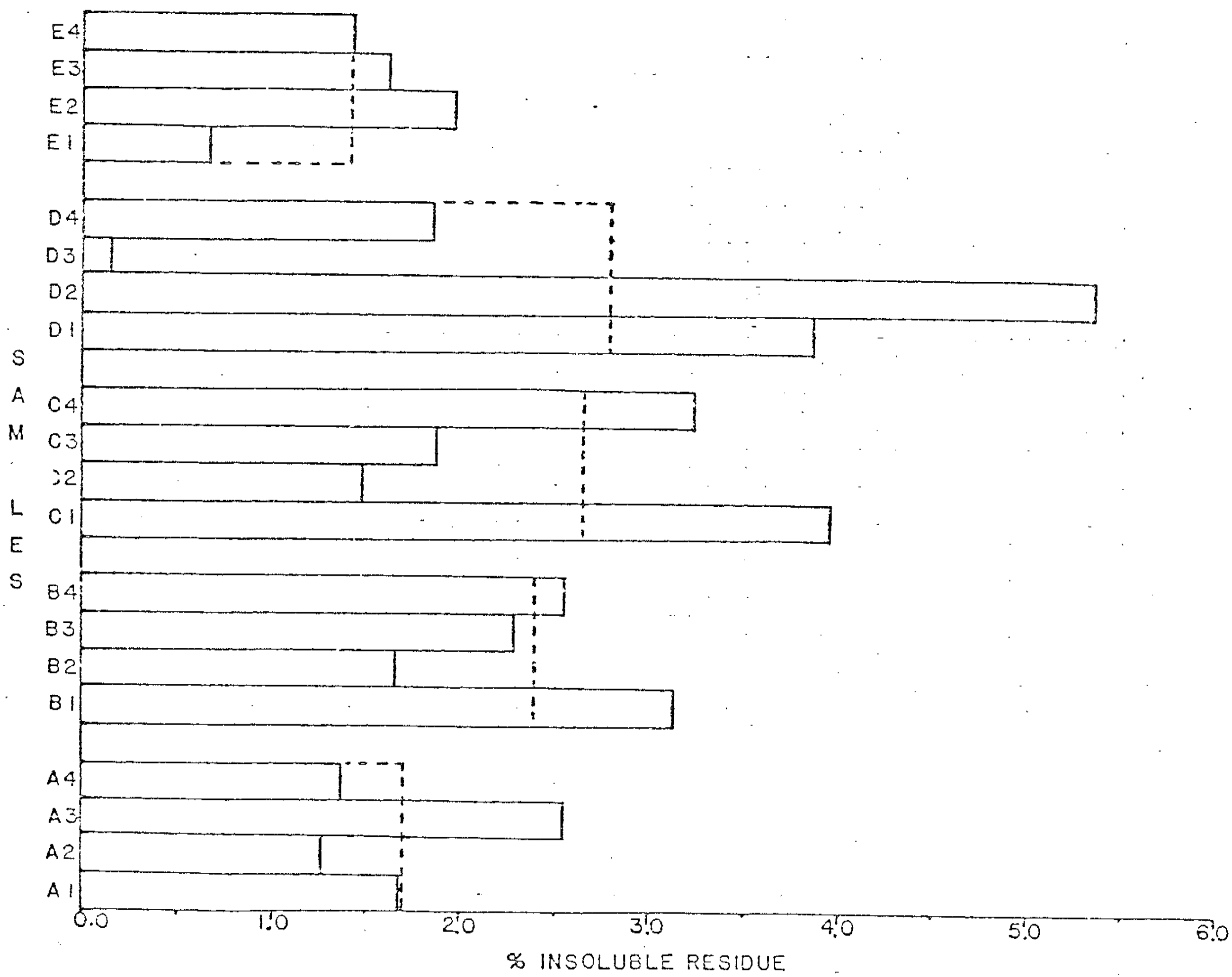

(continued next page)

Fig. 18. (continued)

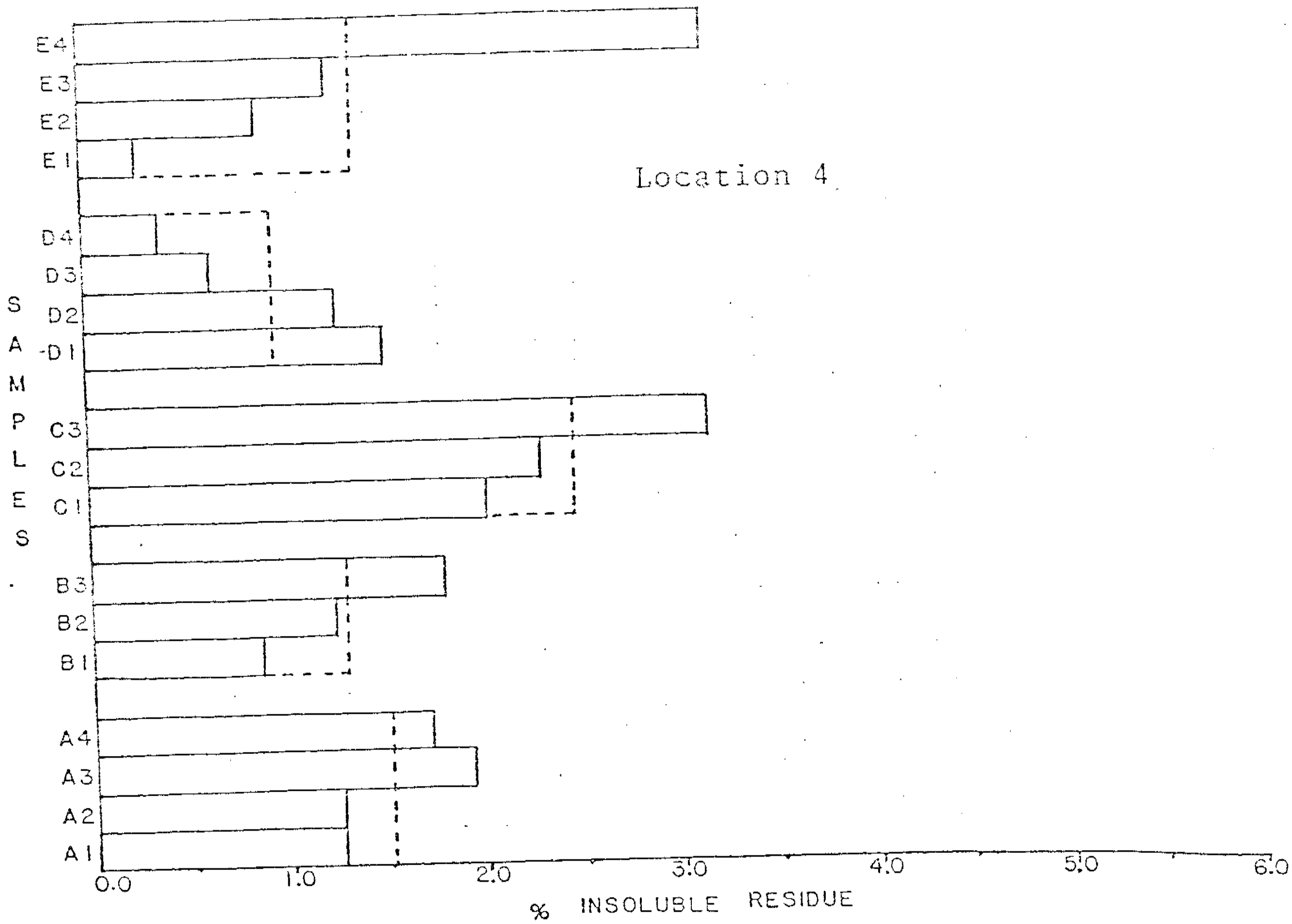

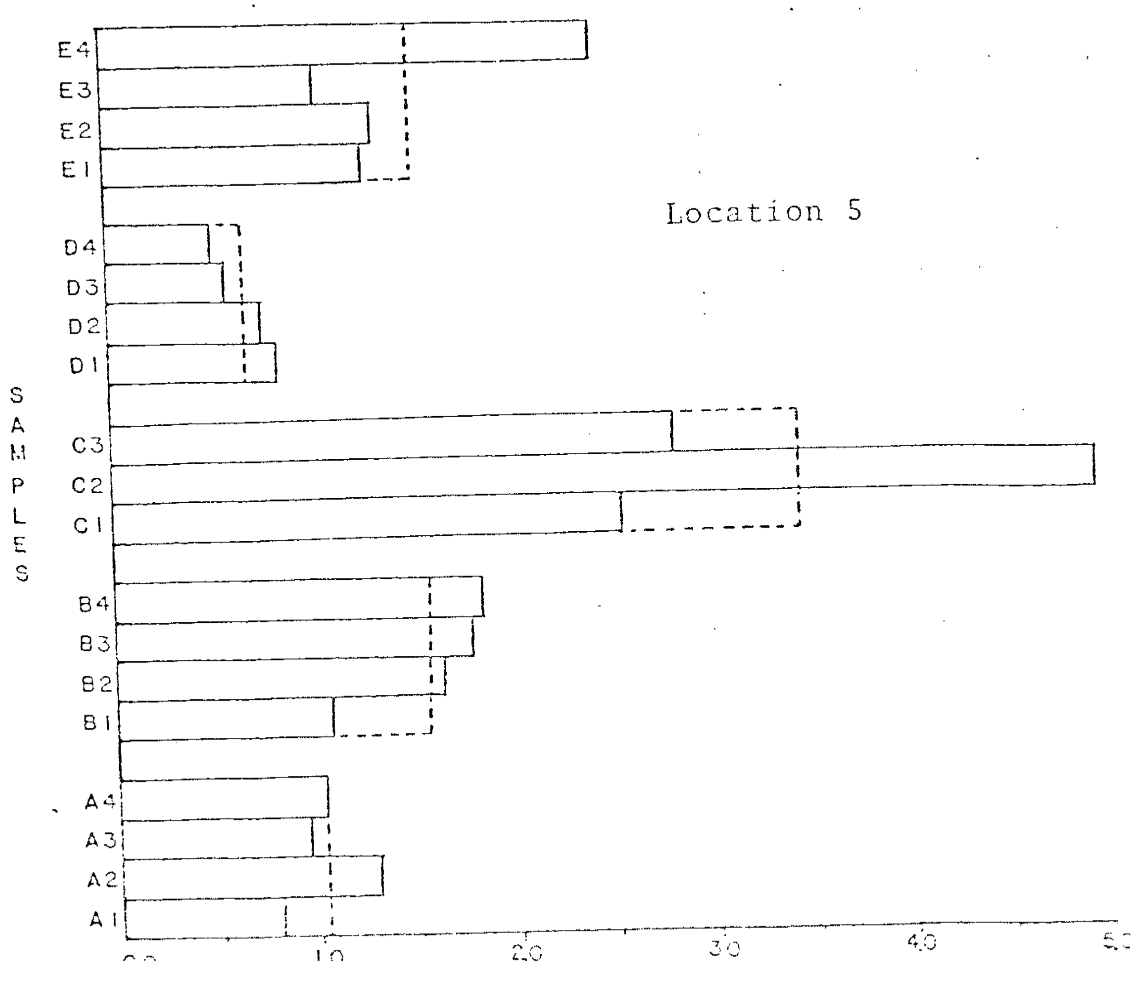

not observed at the western study location. At this location a slight increase occurs across the sample locations B, C, and D.

PETROGRAPHIC STUDY

Five thin sections were made from samples collected across the western trough on the north side of the canyon. These samples represent the same locations studied for insoluble residue. The percentage of intraclasts, ooids, peloids, skeletal material, micrite, neomorphic spar, precipitated spar, terrigenous debris, organic material and pore space was determined by visual estimation and the sequence of diagenetic events formulated.

In general, the percentage of constituents of the five thin sections is similar (Fig. 19). The main differences are found in samples C and D. These differences occur in the percentages of skeletal material, micrite, and neomorphic spar.

The percentage of skeletal material within samples C and D is 40 and 30 percent, respectively, where abraded bryozoan, encrusting and benthic forams, phylloid algae, crinoid columnals, ostracods, brachiopods and pelecypods occur. This contrasts with the 10, 8, and 15 percent in samples A, B, and E, respectively. The skeletal material consists of pelecypods, benthic and encrusting forams, crinoid columnals, bryozoan, echinoid spines, brachiopod

Fig. 19. Plots showing variations in percent constituents vs. bedding zones for study location 3.

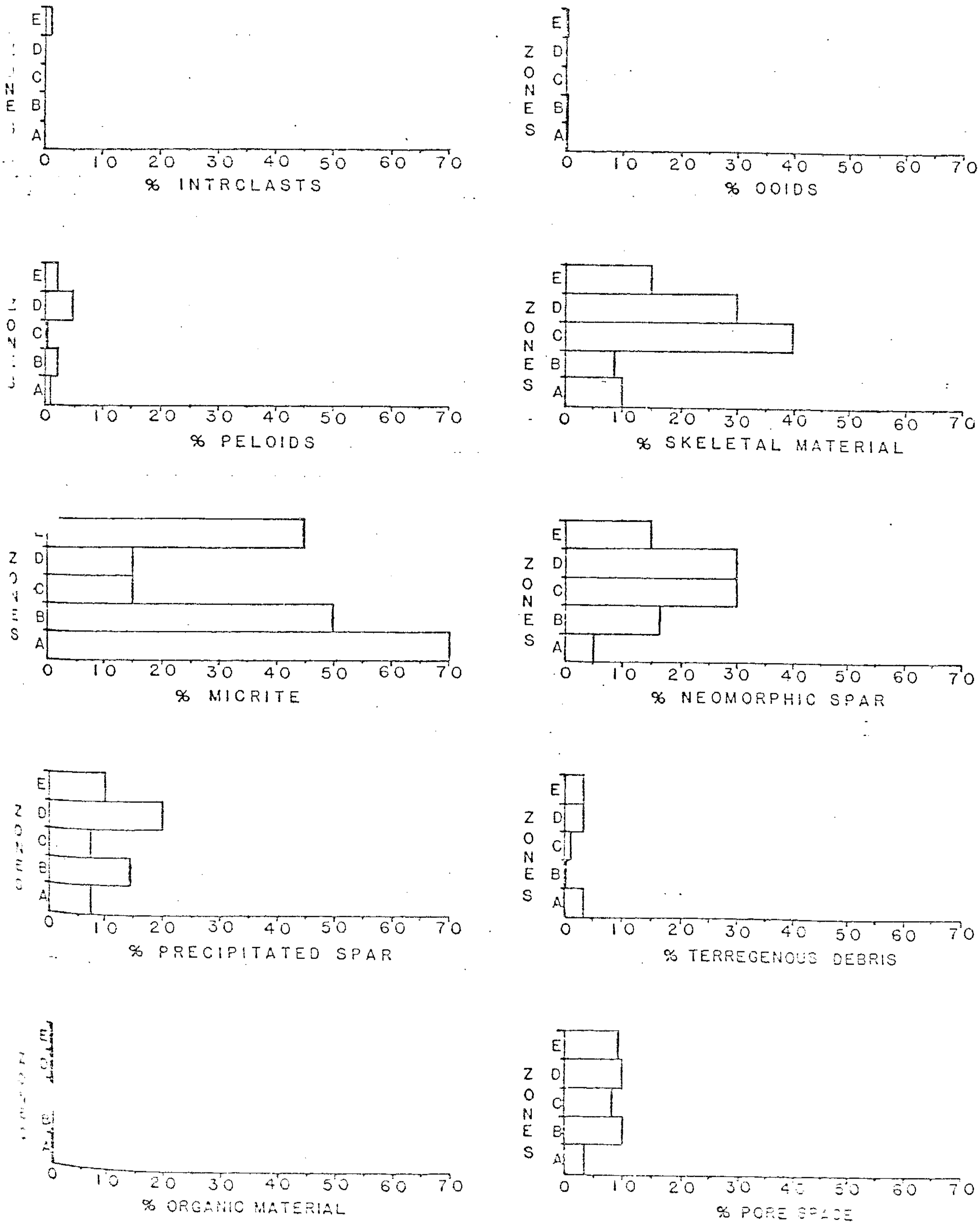

spines, phylloid algae and a trilobite. Micrite envelopes occur on phylloid algae, pelecypods, gastropods and crinoid columnals. Evidence of burrowing is present within all five samples.

The percentage of micrite is greater in samples A, B, and E than in C and D. Samples A, B, and E are composed of 70, 50 and 45 percent micrite, respectively. This compares with 15 percent micrite occurring in both samples C and D.

Neomorphic spar is more abundant in samples C and D than in A, B, and E. In both samples C and D the percentage of neomorphic spar is 30 percent. Microspar occurs throughout samples C and D. In sample D, the occurrence of microspar forms variously shaped pseudo-peloids (Longman, 1980). These have no distinct outline and grade into microspar. For this reason they are not believed to be organic peloids, but rather circular bodies formed by directional neomorphism. Samples A, B, and E contain 5, 16, and 15 percent neomorphic spar, respectively. In these samples both microspar and pseudospar are present. They occur in irregular patches that range in size from 0.3 mm to 4.0 mm. A gradational relationship occurs between the pseudospar and microspar with the surrounding micrite. In sample E pseudo-peloids are also present.

Sequence of Diagenetic Events

The sequence of diagenetic events for all samples follows the same pattern. The first stage of diagenesis took place while the sediments remained in a marine phreatic environment. Within this environment little alteration occurred to the sediments of all the samples. Some micritization of lime mud may have occurred. Micrite envelopes formed on some phylloid algae, crinoid columnals, gastropods and pelecypods and isopachous cement was precipitated in the zooecia of the bryozoan.

The diagenetic environment then altered to fresh water phreatic. It was in this environment where most of the changes in the sediments took place for all samples. In this environment, water undersaturated in calcium carbonate, leached unstable aragonitic pelecypods and algal grains, forming moldic pores. These waters eventually became saturated in calcium carbonate, and equant, drusy and blocky spar was precipitated within burrows, moldic pores, and intraparticle pore spaces with the crystals coarsening toward the center of the pores. Unstable, high Mg-calcite crinoid columnals were replaced at this time by stable, low Mg-calcite. Syntaxial rim cement was then precipitated on these grains. Neomorphism of micrite occurred to varying degrees, possibly depending upon the amount of micritization that took place in the marine phreatic environment. Within samples A, B, and E neomorphism occurred in isolated, irregular patches and along fractures. This compares with samples C and D where micrite was neomorphosed to microspar, throughout. This neomorphism created pseudo-peloids of various shapes.

Summary

The major differences that occur between the zoned and bedded samples are in abundance and diversity of skeletal material, the amount of micrite and the percentage of insoluble residue. Diagenetic environments imposed upon the samples were the same. Samples A and B are representative of the light-gray zone of the previous investigation. Above this zone the black packstone is present. The percentage of insoluble residues within the black packstone decreases toward the west. The significance of these changes will be discussed in the following chapter.

ENVIRONMENTS OF DEPOSITION

A number of depositional environments are represented within the upper Laborcita Formation. These include fan-delta (Holmes, 1965; McGowen, 1970), shoreface, shelf, algal bioherms, lagoon, and interdistributary bay environments. Their recognition is based on physical, chemical, and biological factors.

The strata within the study area are divided by the author into lithosomes. The term lithosome is based on the definition of Moore (1957). This classifies a lithosome as an "independent body of genetically related sedimentary deposits of any sort." Distinctions between lithosomes are based on pronounced changes within the depositional environment. These changes are marked by the occurrence of well defined laterally continuous units. By doing this, three types of lithosomes can be distinguished: 1) carbonate; 2) clastic; and 3) mixed carbonate and clastic. The interpretations of these lithosomes are represented in Plate 2.

The color of the clastic sediments varies from reddish-brown to green. The origin and environmental significance of red coloring within sediments is controversial. Van Houten (1964) points out that red color in sandstones, siltstones, and mudstones is due to the color of the mud matrix or to the color of ferric oxide cement. He considers this to be caused by two cycles of coloration.

The "first cycle" derives its coloration from deep weathering in the source area to supply free ferric oxide. The ferric oxide occurs either in chemical solution or colloidal suspension and acts as a pigment on the sediment. Redbeds may also acquire their coloration by "second cycle" processes. In this process, red beds inherit their color from previously stained red deposits or red minerals.

Upon deposition, "first cycle" sediments that accumulates in oxidizing environments becomes reddish-brown through aging and dehydration of brown ferric oxides. If accumulation occurs in a reducing environment sediments take on a drab color. The role of later diagenesis by ground water is problematical. It is possible that reduced ground water could alter the color of "first cycle" red beds. For this reason, the coloration of clastic rocks will not be used as evidence in the recognition of depositional environments.

The occurrence of glauconite can be used as environmental indicator. Glauconite has been observed to form in marine environments from 5 to 1,000 fathoms (Porrenga, 1967; Triplehorn, 1966; Allen, 1965; Burst, 1958; Galliher, 1935). It forms under reducing conditions by the replacement of colloidal silica, fecal pellets, volcanic glass fragments, organic opaline silica, feldspar, micas, pyroxene, quartz, and calcite (Triplehorn, 1966).

DEPOSITIONAL MODEL

The depositional model put forth by the author for the sequence of alternating clastic and carbonate rocks is a shallow marine shelf environment that was influenced, and at times dominated, by a prograding fan-delta. A fan-delta is an alluvial fan that progrades into a standing body of water from an adjacent highland (Dutton, 1982; Wescott and Ethridge, 1980; Handford and Dutton, 1980; Galloway, 1976; McGowen, 1970) (Fig. 20). The highlands associated with the fan-delta would have then been the Pedernal Uplift, located to the east of the study area. The key to the recognition of fan-delta deposits is the interfingering of coarse-grained clastics and marine sediments (Dutton, 1982).

Fan-deltas have been subdivided into four main depositional environments: fan plain, distal fan, main channels, and prodelta by McGowen (1970) in his study of the Gum Hollow fan-delta of the Texas coast. McGowen also recognized destructional bars on the distal fan. These result from the reworking of fan sediments.

The fan plain is located at the more distal, subaerially exposed part of the fan-delta (Fig. 20). Fan plain sediments comprise most of the exposed fan-delta surface (McGowen, 1970). The fan plain is characterized by shallow braided channels, longitudinal bars, and scour troughs. The dominant sedimentary structures are trough-shaped cross-strata and parallel laminations. Finer

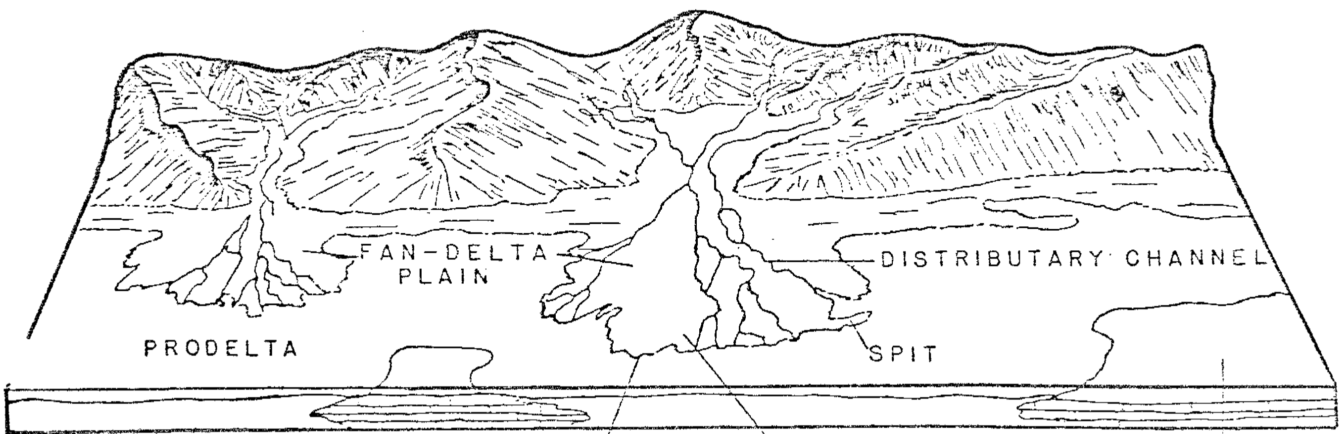

Fig. 20. Schematic diagram of fan-delta system (modified from McGowen, 1970; Handford,1980; Dutton, 1982).

grained sandstones and siltstones are deposited in the fan plain marshes and overbank deposits while coarser grained sandstones and conglomerates are deposited in fan plain channel deposits (Dutton, 1982).

Longitudinal and transverse bars are the most abundant bed forms in the fan-delta braided channels (Wescott and Ethridge, 1980). Channel deposits are distinguished by scour, multiple upward-fining sequences, parallel laminations, and trough-shaped cross-strata (Dutton, 1982). Main channel depositional units are similar to, but thicker than, those deposited on the delta plain.

The distal fan delta (Fig. 20) lies near sea level and extends from the distal end of longitudinal bars on the fan plain to the shoreline (McGowen, 1970) The distal-fan sediments are homogeneous, parallel laminated, or rippled sandstones with thin mud layers (Dutton, 1982). Small, trough sets cross-strata may also be present. Burrows and plant debris are common.

Distal fan deposits are commonly reworked after deposition by longshore currents and breaking waves (McGowen, 1970). Reworked sand may be deposited on the subaerial distal fan as destructional bars, or it may be carried offshore, parallel with the distal fan in spits or offshore bars (Dutton, 1982; Fig. 20 herein). Lagoonal clays may be deposited behind these structures. Reworked terrigenous material may also be deposited in high-energy environments such as oolite shoals and offshore bars on the carbonate shelf. Fossil fragments are commonly mixed with the terrigenous sands. Cross-laminated and parallel laminated sandstones are the most common reworked sediments (Dutton, 1982). Gravel beds may also occur and represent beach deposits that formed when wave attack of the fan-delta margin removes finer grained sediment (Dutton, 1982).

Basinward of the distal fan is the shoreface. The term shoreface is defined as " the submerged seaward side of a barrier (or open coast) extending from the outer edge of a beach to a distinct change in slope (Friedman and Sanders, 1978)." Fine sand with even, subparallel laminations and ripple bedding characterize this zone. Further offshore the sediments consist of parallel laminated, interbedded, fine sands and mud. These grade basinward into megarippled, medium to coarse sand, which is commonly bioturbated (Howard and Reinek, 1972).

It can be seen that many characteristics of the shoreface and reworked distal fan deposits are similar. The difference is in the size of the material. The reworked distal fan contains conglomerate deposits interbedded with finer sediments while the shoreface deposits are restricted to sand size and finer sediments.

The shoreface grades basinward into the prodelta. This environment is characterized by fine-grained muddy sediments. These are mostly laminated clays and silty clays. The sediments become more silty landward. Shell remains are common throughout (Reinek and Singh, 1975).

Carbonate environments associated with fan-deltas include shelf, lagoon, interdistributary bays, and algal bioherms. According to the model developed for the Late Pennsylvanian-Early Permian Mobeetie field of the Palo Duro Basin by Dutton (1982), algal bioherms developed along strike on the shelf and separated the open-shelf environment from a more protected lagoon on the landward side of the bioherms (Fig. 21).

"Carbonates from the open-shelf are dominantly algal-crinoid-foraminiferer (sic) wackestones and packstones. These contain varying amounts of terrigenous silt and mud. High-energy grainstone facies are less abundant and are mainly associated with destructional distal fan-delta-shoreface environments. Oolite grainstones with terrigenous sand and fossil fragment nuclei are common in this setting (Dutton, 1982 p)."

Algal bioherms display a vertical sequence. The base of the bioherm developed on a silty crinoid lagoonal wackestone (Dutton, 1982). This is overlain by a sequence of phylloid algal wackestone core, foraminiferal or encrusting algal boundstone crest and algal-foraminiferal packstone to grainstone flanking beds (Ginsburg, et al. 1972; Wilson, 1975; Fig. 22 herein).

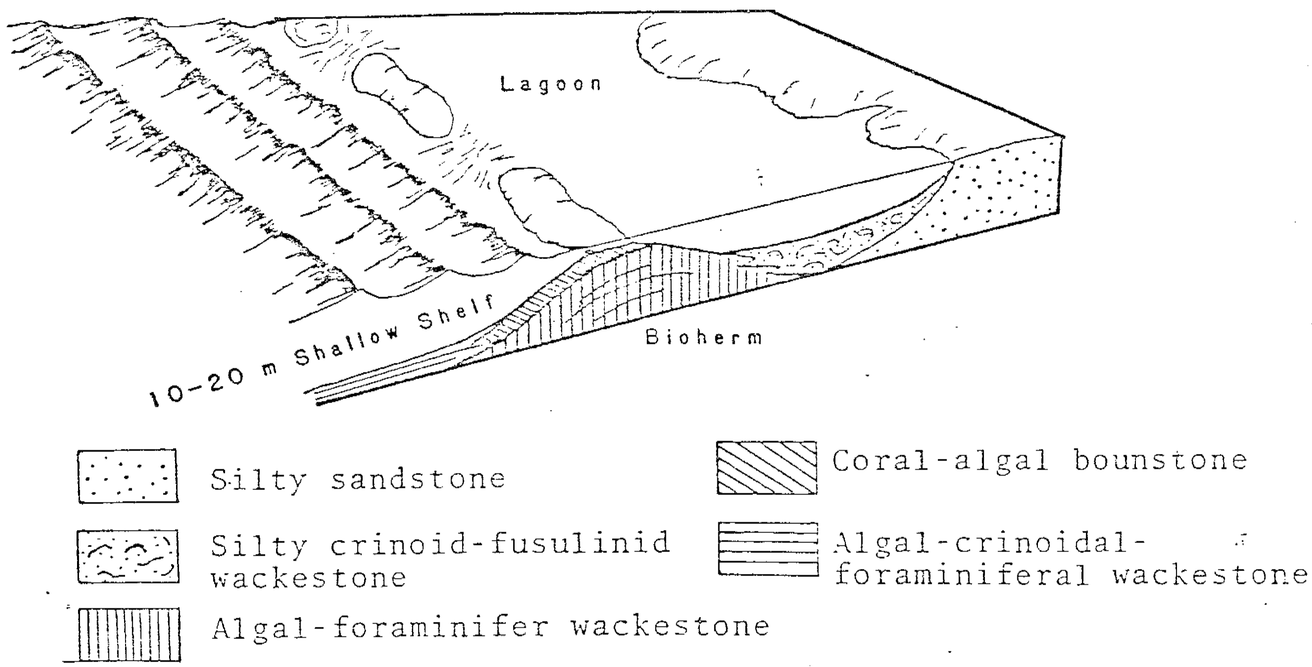

Fig. 21. Schematic block diagram showing model for bioherm development (modified after Wilson,1975, Dutton, 1982)

"Lagoonal deposits generally consist of crinoid-fusulinid wackestones with varying amounts of silt and mud. Shale partings, wavy laminae, and burrows are common. Faunal diversity is low, but solitary rugose corals, and brachiopods are locally present (Dutton, 1982, p.)."

Interdistributary bays occur between fan-delta lobes. These deposits consist of silty mudstones, wackestones and packstones. They are homogeneous and contain shale partings and burrows (Dutton, 1982). Interdistributary bay sediments are similar to the open-shelf and carbonate lagoon sediments, but because of the periodic influence of fresh water from the fan-delta, they tend to have a more restricted fauna.

INTERPRETATIONS

The lowest lithosome in the study area is carbonate. It is composed of sandy mudstone, sandy, fossiliferous wackestone, sandy, rounded intraclastic packstone and oncolitic packstone. These are continuous across the map area. The occurrence of sand and shale partings within the lower portion of this lithosome suggests the proximity of a clastic source and the presence of currents to transport these sediments. Wave action could not have affected this environment because it would have caused the winnowing of clays and lime mud. These conditions are found in the intertidal zone. As the lithosome accumulated the environment changed, allowing brachiopods, pelecypods, gastropods, sponges, and rugose corals to flourish. The presence of filter feeding sponges and corals suggest nonturbid conditions. This type of environment is found within the subtidal zone. With continued deposition conditions changed again to one in which intraclasts were eroded, transported, and deposited with sand and lime mud. This change indicates a transition from an environment unaffected by tidal-currents to one dominated by them. In this environment periodic subaerial exposure of the sediments would allow mud cracks to form, which could easily be ripped up and transported by tidal currents. The roundness of these intraclasts indicate some degree of transport and abrasion occurred. The last depositional environment represented in this lithosome is one in which oncolites were formed. Studies into the environmental significance of stromatolitic growth forms at Shark Bay, Australia, by Logan, Rezak, and Ginsburg (1964), have found that oncolites are formed in the low intertidal to subtidal zone, where water agitation is more constant. These waters would be nonturbid because the presence of fines in the water would inhibit algal growth. Cyclic changes can, therefore be recognized within this lithosome. These changes are seen by the transition between intertidal and subtidal zones. The types of depositional environments where these changes occur are along landward margins of a shallow shelf, interdistributary bay or carbonate lagoon.

The presence of a relatively diverse fauna within the wackestone suggests more normal marine conditions found on the shelf, rather than in a restricted lagoon or interdistributary bay (Fig. 23, p 99).

This carbonate shelf lithosome is overlain by a clastic lithosome. This clastic lithosome is composed of conglomerate, arkose and siltstone. (See pages 11, 12, 21 and 35.) This fining upward sequence from grain-supported conglomerate to arkose and siltstone can be found in the fan plain, distal fan, or shoreface. The lack of distinct erosional channels, coal marshes, and overbank siltstones and fine sands discounts the possibility of a fan plain environment. This leaves either the distal fan or shoreface. Along the seaward margin of the distal fan wave action may attack the fan, winnowing away the fines and leaving a grain-supported gravel beach (Runchin, 1958). With a decrease in wave action caused by an increase in water depth, less sands would be winnowed and the clasts would become matrix supported. Further offshore only sands would be present. These sands would grade basinward into silts. This type of transition is envisioned for this lithosome and therefore represents the appearance of a reworked distal fan and shoreface environment on the underlying carbonate shelf. The greater thickness of units to the north and decrease in the amount of conglomerate to the south suggests that the location of the delta was to the northeast (Fig. 23, p 99).

This clastic shoreface lithosome is overlain by a carbonate lithosome composed of mudstone and sandy, fossiliferous wackestone. (See pages 12, 21 and 35.) The occurrence of silt at the base of the mudstone depicts the transition of the underlying shoreface into a carbonate environment. After the initial change only clays were brought into the environment. This is seen by the occurrence of shale partings, and implies a relatively quiet environment. The waters gradually became more agitated and sands were transported into the area, inhabited only by ostracods and burrowing organisms. Symmetrical ripple laminations formed in the north, indicating the presence of oscillatory tidal currents (Harms, 1969). These conditions can be found within a carbonate lagoon or interdistributary bay. A shelf environment is discounted by the very low biotic diversity. According to Dutton (1982) one would expect to find crinoids and forams as the dominant organisms living within a carbonate lagoon. In this carbonate lithosome, only ostracods are present. Ostracods may live under a very wide range of conditions ranging from fresh water to hypersaline (Heckel, 1972). For this reason they are not a good indicator of environmental conditions. However the absence of marine organisms suggests the possibility of an interdistributary bay where the waters are seasonally influenced by fresh water from the fan-delta. This is supported by the occurrence of a reworked distal fan and shoreface facies below this lithosome. For these reasons it is concluded that this lithosome represents an interdistributary bay (Fig. 23, p 99).

Overlying this carbonate interdistributary bay lithosome is a clastic lithosome composed of siltstones, arkoses and conglomerates. The conglomerates occur only in the southern section. (See pages 12, 22, 35, 36 and 37.) The presence of a fining upward sequence from arkose to siltstone in the northern and central sections indicates a decrease in hydraulic energy. Water in this environment is believed to be marine due to the occurrence of whole pelecypods and micrite. These characteristics are found within the shoreface. A fan plain environment is discounted because of the lateral continuity of beds and presence of whole shells. In the southern section conglomerates are interbedded with arkoses and shales. Multiple upward fining sequences within this section suggest deposition either in braided distributary channels or a reworked distal fan-shoreface. Deposition in a fluvial environment is refuted because of the presence of carbonates both above and below this lithosome. As distributary channels pass across the fan plain the flow velocity decreases and channels become shallower and less erosion takes place. Eventually, the channels cross the distal fan and enter the marine environment and are mixed with the shoreface and reworked distal fan deposits. It is this type of setting envisioned for the southern part of the lithosome. This is postulated because of the absence of a distinct erosional channel and lack of imbricated clasts. The presence of angular mudstone clasts within conglomerates supports the idea of the transition of channels into a marine environment. This is further supported by the occurrence of interdistributary bay facies below this lithosome and indicates the return of a fan-delta lobe into the area (Fig. 23, p 99).

This clastic, shoreface-reworked distal fan-channel lithosome is overlain by a carbonate lithosome composed of mudstone and wackestone. (See pages 12, 22, and 37.) Within this lithosome sands and clays were incorporated with the lime mud by tidal currents. These same currents created ripple cross-laminations. Within this environment ostracods, pelecypods, and burrowing organisms lived. Pelecypod shells were abraded after death. These characteristics may represent either a carbonate lagoon or interdistributary bay. Pelecypods, like ostracods, may inhabit marine to fresh water environments, and are not good environmental indicators. The absence of strictly marine organisms particularly crinoids and forams suggest marine waters periodically influenced by fresh waters. These conditions are found in an interdistributary bay, rather than restricted marine waters found in a carbonate lagoon. The occurrence of this lithosome intertonguing with the underlying migrating fan-delta lobe in the southern section strongly supports this conclusion. The increase in thickness of this lithosome is believed due to the intertonguing (Fig. 23, p 99).

Overlying this carbonate interdistributary bay lithosome is a clastic lithosome composed of siltstone, noncarbonate mudstone, subarkose, and arkose. (See pages 13, 22 and 37.) The interbedding of arkose, siltstones and noncarbonate mudstone within this lithosome indicates variation in hydraulic energy. The homogeneous to laminated nature of the arkose suggests deposition rather than erosion and transport as the major activity occurring in the area. These characteristics may be found in fluvial, fan plain, or shoreface environments. The existence of an interdistributary bay below and carbonates above this lithosome discount the possibility of a fluvial environment. The absence of any evidence of erosion, such as channels or scour troughs along with the lateral extent of the units implies a shoreface rather than fan plain environment. Siltstone and noncarbonate mudstone infers deposition in the deeper portion of the shoreface, near the transition to shelf sediments (Fig. 23, p 99).

A mixed carbonate and clastic lithosome overlies this clastic, shoreface facies. This lithosome is composed of mudstone, packstone, siltstone, and arkose. (See pages 13, 22, 23, 37 and 39.) The presence of sand in the carbonates and the interfingering of siltstones and arkoses in this lithosome indicate a transition from a carbonate to a clastic environment. The carbonate environments that could be represented are lagoon, interdistributary bay and shelf. The interfingering of clastics detracts from the lagoonal interpretation because carbonate lagoons are formed during times of very low clastic influx when carbonate barriers are able to form. Previously the biota within an interdistributary bay was restricted to ostracods and pelecypods. In this environment brachiopods, pelecypods, bryozoa and a stromatolite-like organism lived. Of these, brachiopods and bryozoa are restricted to the marine environment. For this reason along with the relatively high diversity of the biota, normal marine conditions are depicted, indicating a shelf environment. This shelf environment interfingers with the shoreface represented by siltstone and arkoses. This conclusion of a shelf-shoreface environment is supported by the presence of a shoreface environment in the lithosome below (Fig. 23, p 99).

Overlying this mixed shelf-shoreface lithosome is another mixed carbonate and clastic lithosome. Clastics dominate this lithosome which is composed of subarkose, shale and oolitic packstone. (See pages 14, 23, 25 and 39.) The most striking characteristic within this lithosome is the change in dip direction of the wedge-sets in the subarkose. The change in directions from east to west indicates two depositional trends. Landward the subarkose interfingers with and is divided by shale. This relationship may be found in fan plains associated with marshes or on a barrier bar or island associated with a clastic lagoon. The occurrence of an oolitic packstone interbedded with the arkose indicates agitated marine conditions as seen on the Bahama Banks by Newell, Imbrie and others (1959). This places the environment of deposition along a barrier bar or island with its associated lagoon. This is supported by the occurrence of symmetrical ripple marks which indicate the presence of oscillatory waves or currents (Harms, 1969). This environment ended with the migration of the barrier over the lagoon. This is seen by the presence of eastward dipping wedge-sets above the shale and the occurrence of carbonates above this lithosome (Fig. 23, p 99).

A carbonate lithosome overlies this mixed barrier and lagoon facies. This lithosome is composed of wackestones and packstones. (See pages 14, 25, 39 and 40.) The appearance of two intraclastic packstones within this lithosome indicates cyclic facies changes within this environment. The basal sandy wackestone shows a transition from the previous barrier environment. As the new environment became established, periodic exposure allowed rectangular intraclasts to be ripped up and transported by tidal currents. This occurs in the intertidal zone. The environment changed and ooids and disarticulated crinoid columnals were the only grains transported into the area. This along with the increase in the percentage of lime mud being deposited suggests less agitated conditions found in the subtidal zone. The environment then returned to the intertidal zone seen by the return of the intraclastic packstone. The types of environment where the transition from subtidal to intertidal zones may occur are in the interdistributary bay, shelf or lagoon. The absence of fan-delta sediments associated with this lithosome detracts from the possibility of an interdistributary bay. Within a shelf environment the normal marine waters would allow a relatively diverse fauna to be present. This is not seen in this lithosome. Instead only crinoids are present. Therefore a lagoonal environment is postulated for this lithosome. This conclusion means that there should be a carbonate barrier of some sort to the west of the study area (Fig. 23, p 99).

This carbonate lagoon facies is overlain by a mixed clastic and carbonate lithosome, composed of subarkoses, a sponge packstone and a stromatolitic wackestone. (See pages 14, 16, 25, 26 and 40.) The occurrence of a sponge packstone within this dominantly clastic lithosome indicates the transition between a carbonate and a clastic environment. This type of transition may occur along a shoreface or reworked distal fan. The absence of any conglomerates and the lateral continuous nature of the units detract from a reworked distal fan conclusion. This leaves a shoreface environment for the deposition of the clastics. Within this environment the coarsening upward of the basal subarkose shows an increase in hydraulic energy. This increase culminated before the deposition of fragmented sponges and represents progradation of the shoreface onto the underlying lagoon. This was followed by a rapid retreat of the shoreface and deposition of the sponge packstone and stromatolitic boundstone. Progradation of the shoreface was reinitiated with the deposition of siltstones followed by subarkoses. These changes may be due to either tectonic movements, subsidence of the underlying strata or eustatic changes in sea level (Fig. 23, p 99).

Overlying the mixed shoreface facies is a carbonate lithosome, composed of sandy wackestone, fossiliferous, intraclastic packstone, black, fossiliferous packstone, algal packstone, intraclastic, foraminiferal packstone, fossiliferous packstone and crinoidal packstone. (See pages 16, 26, 27, 40, 41, 55, 57, 58, 59, 64, 66 and 68.) The basal wackestone of this lithosome contains a marine fauna of blue-green algae and brachiopods. These organisms may be found in either a lagoonal or shelf environment. The presence of blue-green algae creating horizontal laminations indicates subtidal conditions (Heckel, 1972). Conditions changed within the environment and a fossiliferous, intraclastic packstone was deposited. The occurrence of a relatively diverse fauna within the packstone suggest normal marine and therefore shelf conditions for the underlying wackestone.

Within the fossiliferous, intraclastic packstone, the gradation from brownish-gray to light-gray, accompanied by the increase in the percentage of insoluble residue, micrite and skeletal material suggests changes in conditions occurred within this new environment. This can be seen by considering the stages of bioherm development.

The first stage begins with the proliferation of phylloid algal plates. These plates were piled up by wave action, causing shoaling on the shallow shelf. This mechanism has also been postulated by Wilson (1975) for the creation of Virgilian algal bioherms. Shoaling may be either caused by transgression or regression. The occurrence of a sand within the basal wackestone suggests the proximity of a clastic shoreface. This implies initial transgressive shoaling and is supported by the idea that regressive shoaling would tend to destroy the mound. As the algal mounds developed, radial fan aragonite needles grew within shelter pores. This helped to bind and support the bioherm. Eventually the environment began to change from one that favored the growth of phylloid algae to one that favored a more diverse biota. This can be accomplished by deepening the environment below a depth favorable for the growth of phylloid algae. As the depth increased, lime mud would no longer be winnowed away and free standing bryozoa and crinoids could live. Deepening of the environment could have been caused by either compaction and subsidence of the underlying strata, tectonic movement or eustatic changes in sea level.

Growth of the bioherm can therefore be divided into two stages. The first stage is characterized by transgressive shoaling. Wave action during this stage caused the winnowing of lime mud. As transgression continued, the environment deepened below the critical depth limit for optimum phylloid algal growth. At this time a second stage began with the colonization of the bioherm by bryozoa, crinoids, forams, brachiopods, pelecypods, gastropods, and ostracods. Lime mud and clay were no longer winnowed away by wave action. The second stage ended with an abrupt return to shallower conditions that favored the growth of phylloid algae. The abruptness is seen by the sharp contact between the top of the light-gray zone and the bottom of the brownish-gray zone. The cause of this sudden change in depth may be due to tectonic movement or eustatic changes in sea level. The abrupt return to shallow conditions suggest tectonic movement to be the more likely.

These same stages with the addition of a initial pioneer stage were recognized by Toomey and Cys (1979). During this stage "...digitate-shaped plumose colonies of probably blue-green algae and encrusting algae..." (Toomey and Cys, 1979) constructed small irregular mounds with no more than a few centimeters of relief. These mounds formed on a muddy, open marine shelf.

The change in bedding that occurs above the uppermost light-gray zone indicates another change in conditions on the bioherm. This is most noticeable within the black packstone. The decrease in the amount of insoluble residue and the occurrence of chert pebbles to the west indicate an increase in hydraulic energy in that direction and a return to shallow conditions. The hydraulic energy could be in the form of either wave or current action. A crinoidal packstone is present at the top of this bedded sequence. The crinoids are articulate and occur with pelecypods, brachiopods and gastropods. The articulate nature of the crinoids implies quiet conditions. This may be found on the subtidal shelf or in a protected lagoon. The fragmented nature of the other skeletal material suggests the close proximity of abrasive wave action. For this reason along with the occurrence of the bioherm indicates protected lagoonal rather than shelf conditions.

The above lithosome exhibits the algal bioherm sequence of Ginsburg et al. (1972) and Wilson (1975) (Fig. 22). The lower sandy wackestone represents the basal wackestone. This is overlain by the bioherm core indicated by the zoned, fossiliferous, intraclastic packstone. The bedded sequence of intraclastic, fossiliferous packstone, algal packstone, intraclastic, foraminiferal packstone, and fossiliferous packstone represents flanking beds. These flanking beds are overlain by a lagoonal crinoid packstone. This indicates progradation of the bioherm complex (Fig. 23, p 99).

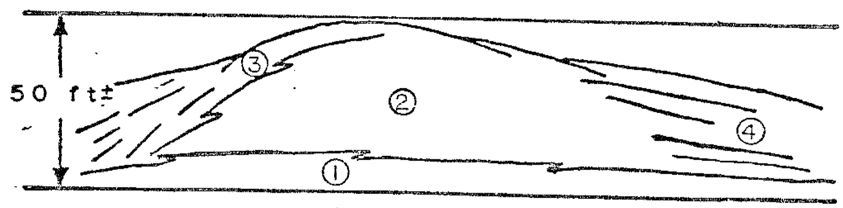

1. Basal wackestone
2. Bioherm core: phylloid algae wackestone
3. Bioherm crest: foraminiferal or encrusting
4. Flanking beds: algal boundstone
   algal-foraminiferal packstone
   to grainstone

Fig. 22. Idealized bioherm sequence (modified after Ginsburg et al., 1972; Wilson, 1975).

Onlapping the eastern side of the bioherm complex is a mixed lithosome composed of shales and interbedded packstones. (See pages 16, 27 and 41.) This lithosome pinches out on the side of the bioherm. Shales interbedded with fossiliferous packstones may occur either in a lagoon with the bioherm acting as a barrier or in a prodelta. Lagoonal waters are more restricted than those associated with prodeltas. For this reason the fauna within lagoons is also more restricted. The biota present within the packstone is relatively diverse. This detracts from the possibility of a lagoonal environment but does not disprove it. North of the study area this lithosome overrides and surrounds a stratigraphically equivalent bioherm. This further disproves the possibility of the bioherm acting as a barrier. Therefore a prodelta is concluded to be the environment on which these shales and interfingering packstones were deposited (Fig. 23, p 99).

Overlying the mixed prodelta lithosome and onlapping the eastern side of the bioherm complex, is a mixed clastic and carbonate lithosome, composed of arkoses, subarkoses, siltstones along with sandy, fossiliferous wackestones and packstones. (See pages 17, 27, 29 and 43.) This mixed lithosome represents a transition between clastic and carbonate environments. The clastic environment may represent either a reworked distal fan or a shoreface, while the carbonates may represent either a interdistributary bay or a lagoon or shelf environment. The lack of conglomerates discounts a reworked distal fan. This is supported by the abundance of micrite in the carbonate, which would not be expected to be associated with a distal fan under attack by waves. The presence of a relatively diverse fauna containing marine brachiopods and forams, discounts both the more restricted interdistributary bay and lagoonal environment. For these reasons a transition between the shoreface and shelf is postulated for this lithosome. This is supported by the decrease to the east (landward) in the amount of carbonates and the presence of a prodelta below and a carbonate lithosome above this lithosome (Fig. 23, p 99).

This mixed shelf-shoreface lithosome is overlain by a carbonate lithosome, which consists of light-gray, sandy, fossiliferous wackestones and packstones. (See pages 17, 29 and 43.) The presence of sand within this wackestone shows the transition from the underlying shelf-shoreface environment. Within this new environment pelecypods, crinoids and ostracods lived. Of these, only crinoids are restricted to marine waters. This new environment could have been either a lagoon or shelf. The relatively diverse fauna, although not indicative of normal marine waters, implies these conditions. This, along with the presence of shelf-shoreface environment below this lithosome, suggests a return to shelf conditions rather than lagoonal (Fig. 23, p 99).

Overlying this carbonate shelf lithosome is a clastic lithosome composed of laterally continuous siltstone and subarkose. (See pages 18, 30 and 45.) The coarsening upwards sequence within this lithosome indicates an increase in hydraulic energy. At the beginning of this increase the sediment was burrowed. Burrows may be found either on the distal fan or in the shoreface. Their occurrence directly above a carbonate shelf lithosome suggests the transition from a shelf environment to a shoreface. The increase in grain size indicates the progradation of the shoreface. Local occurrence of siltstones at the top of this lithosome and carbonates above it represents the shoreface's eventual retreat (Fig. 23, p 99).

Overlying this clastic shoreface lithosome is a carbonate lithosome composed of sandy, fossiliferous wackestone, sandy, fossiliferous packstone and sandy grainstone. (See pages 18, 30 and 45.) The presence of sand within this lithosome indicates the need for a transporting agent within the environment of deposition. This transporting mechanism increased in strength eastward as seen by the transition from wackestone to packstone and into grainstone. This suggests wave rather than current action was the vehicle of transport. This conclusion is supported by the fragmented nature of the fossils. For this reason the environment of deposition could not have been a protected lagoon and it is unlikely that it was an interdistributary bay. This is because wave energy is decreased by refraction around delta margins. The above conclusions lead to a shelf environment, within the breaker zone, and very near shore. This is supported by the occurrence of a shoreface environment underlying this lithosome (Fig. 23, p 99).

This carbonate nearshore-shelf lithosome is overlain by a clastic lithosome, composed of siltstones and subarkoses. (See pages 18, 30, 32, 45 and 46.) The upward coarsening from siltstone to subarkose in this lithosome can be found in either a shoreface or distal fan environment. The presence of symmetrical ripple marks indicates oscillatory transport of the sands. Eventually whole pelecypods, gastropods and nautiloids were deposited in the subarkosic sediments along with chert pebbles. The presence of nautiloids suggests that this environment was at least connected with normal marine waters and that relatively strong hydraulic energy was present to transport the chert pebbles. These conditions formed an offshore bar seen by the rapid decrease in thickness of the subarkose to the east. Behind this bar the hydraulic energy dissipated and medium grained sand was deposited and burrowed. Eventually these conditions prograded over the bar. Progradation of this environment was eventually reversed as indicated by the local occurrence of siltstones at the top of this sequence and the presence of carbonates above this lithosome. Changes like these may be found in the shoreface and along the reworked margins of a distal fan. The lack of cobbles within this lithosome weakens the possibility of a reworked distal fan. For this reason it is concluded that these clastics were deposited with the shoreface environment (Fig. 23, p 99).

This clastic shoreface lithosome is overlain by a carbonate lithosome, composed of mudstones and an overlying sponge buildup. (See pages 19, 32 and 46.) The local occurrence of sand at the base of this lithosome and the presence of a sponge buildup at the top indicate a transition from the underlying shoreface to normal marine conditions in which calcium carbonate production could dominate. This carbonate environment could occur in either a lagoon or shelf. The lateral continuity of the sponge buildup indicates uninterrupted conditions, not found in a lagoon bisected by tidal channels. This points to the shelf as the depositional environment for this lithosome (Fig. 23, p 99).

Overlying this carbonate shelf facies is a slightly mixed clastic and carbonate lithosome, composed of minor amounts of conglomerate, arkoses, siltstones and sandy, fossiliferous wackestone. (See pages 19, 32 and 46.) Coarsening upward within this lithosome indicates an increase in hydraulic energy. The energy became great enough to transport and deposit cobbles. This type of sequence can be found within the shoreface or reworked distal fan. The occurrence of interbedded sandy wackestone indicates the temporary decrease in hydraulic energy. The end of this depositional environment was characterized by a gradual decrease in hydraulic energy marked by the return of silty sediments into the area. This cyclic change in hydraulic energy is most easily accomplished to such a lateral extent within the shoreface. Cyclic changes were caused by the advance and retreat of this environment. The occurrence of the cobble lenses suggest the proximity of a distal fan (Fig. 23, p 99).

This mixed shoreface facies is overlain by a carbonate lithosome, composed of stromatolitic wackestone, algal packstone and fossiliferous wackestone. (See pages 19, 20, 32, 33 and 46.) The relatively diverse biota indicates normal marine conditions found on the shelf rather than in a lagoon. This sequence represents Ginsburg et al.s (1972) and Wilson's (1975) bioherm complex. A biostrome complex is another possibility, because of lack of preservation. Within this sequence the stromatolitic wackestone represents the basal unit. This is overlain by the core represented by the algal packstone. The upper fossiliferous wackestone depicts the flanking beds and lagoon. The small scale of this bioherm may be due to either the degree of its original development or to the preservation of only back margin. The later possibility is the most likely. If the main body of this bioherm has been eroded it would have occupied the same lateral location as the older bioherm. The occurrence of dissolution vugs may represent the effects of the prograding

Abo redbeds. This algal mound-lagoon lithosome marks the top of the Laborcita Formation in the study area.

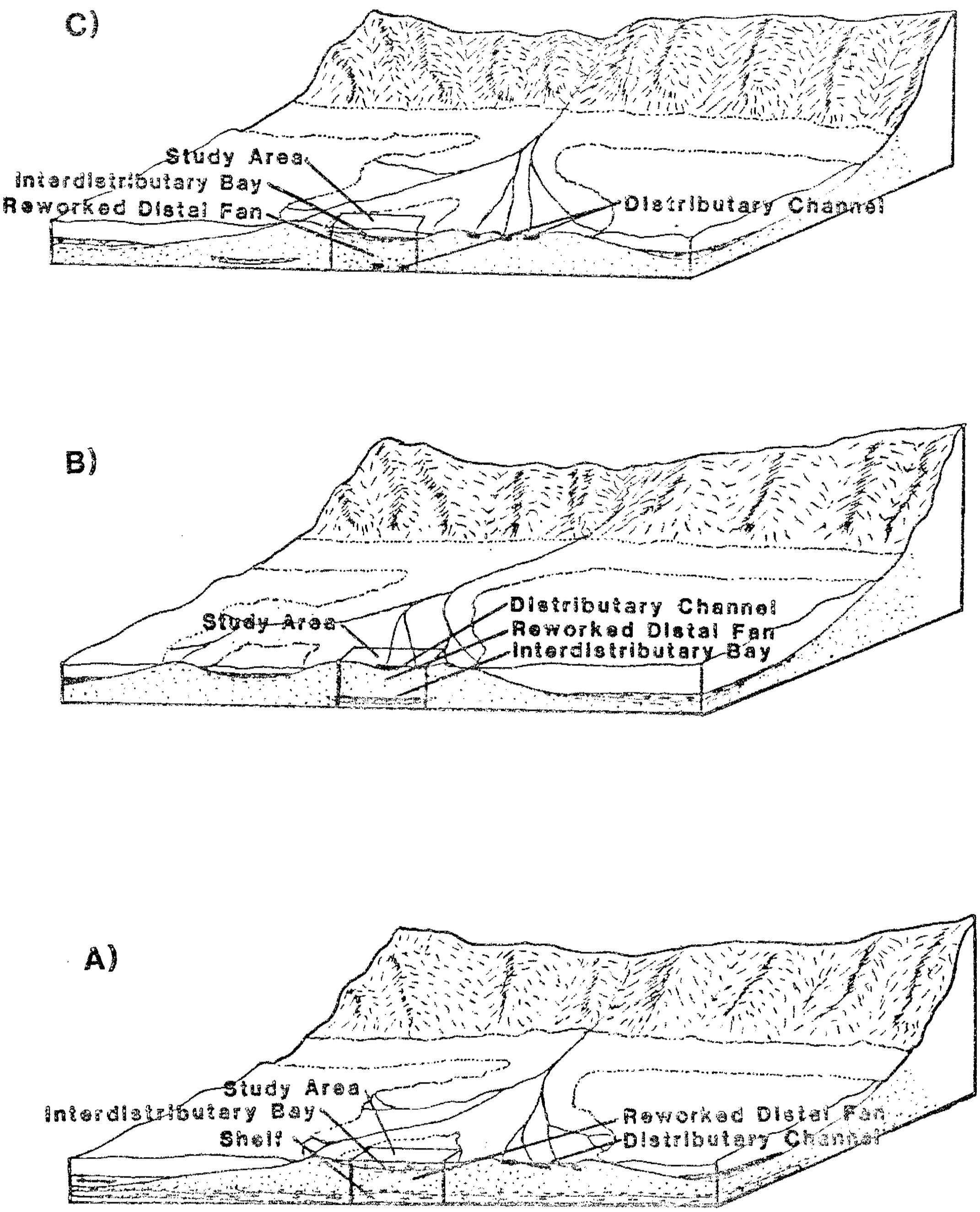

Fig. 23. Idealized block diagrams A (oldest) to F (youngest) showing the location of the study area within the developing depositional system. Lowest environment depicted in the diagrams represents the uppermost environment of the previous diagram. Color represents lithology: blue - carbonate, yellow - sandstone, red - conglomerate, brown - siltstone/shale.

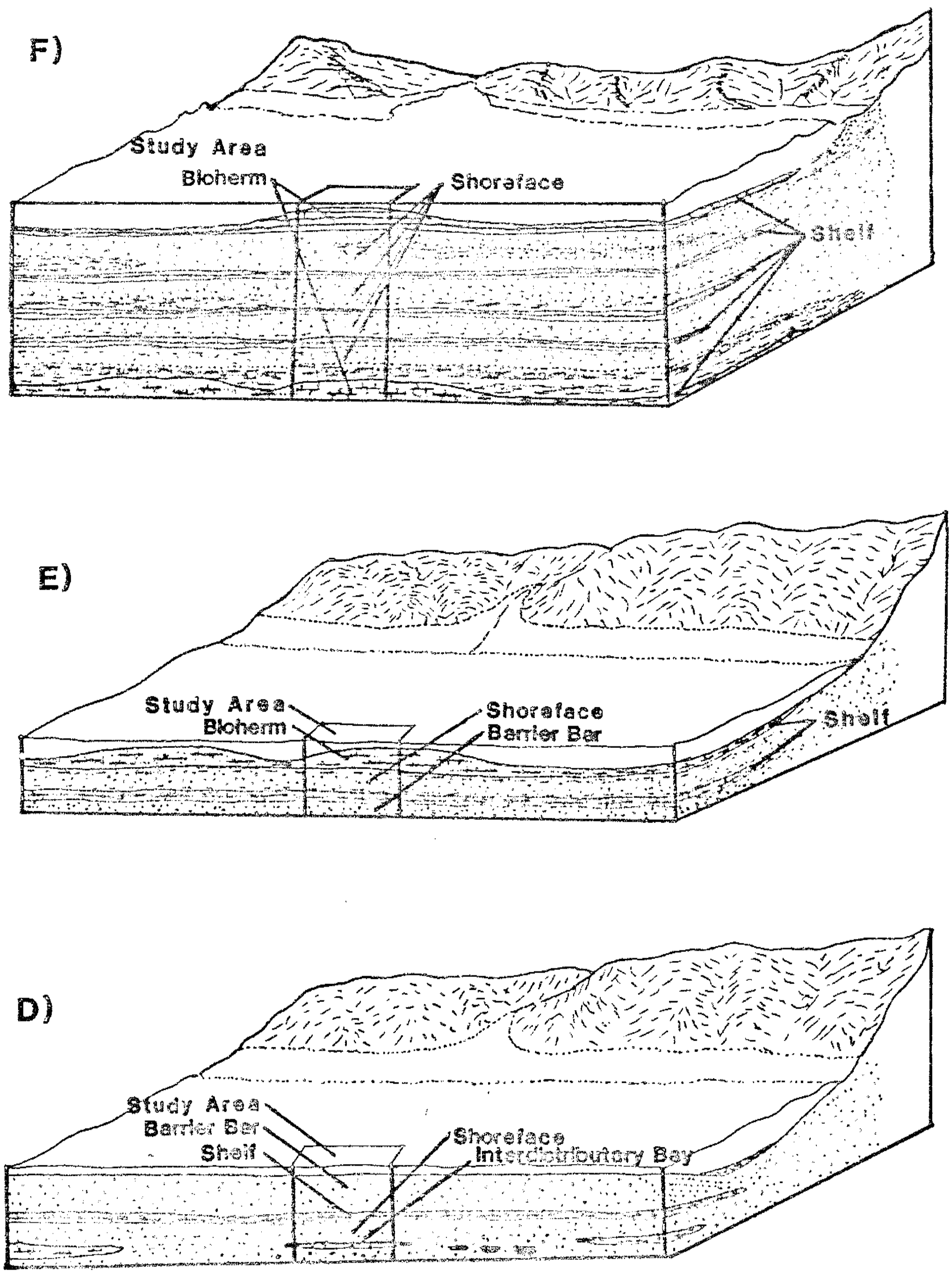

Fig. 23. Continued

Post Laborcita Geologic History

Two diabase dikes were intruded into the Laborcita Formation. These are located at the mouth of the central canyon and along the east-west hill trending eastward from the backside of bioherm. They both are between one and two feet (0.3-0.6 m) wide and nearly vertical. The strike of both dikes is N45E. Otte (1959) believes these dikes may be related to the Tertiary intrusives in the Capitan quadrangle.

Faulting also occurred in this area. One of these faults occurs along the southern side of the central canyon (Fig. 24). This fault trends N55E and dips 59 degrees to the northwest at the mouth of the canyon. The orientation of the fault changes toward the east where it trends N67E and dips 56 degrees southwest. There is seventeen feet (5.1 m) of vertical displacement on this fault. South of this fault in the southern canyon a second fault is present. This fault has a trend of N45E and is nearly vertical. Vertical displacement on this fault is twenty-five feet (7.6 m).

The change in dip direction of the fault in the central canyon may be due to a postulated fault that trends southeast. This fault is postulated because of lateral displacement seen along both dikes. Right lateral movement of four and seven feet (1.2 and 2.1 m) is seen on the central and southern dikes, respectively. If there is a

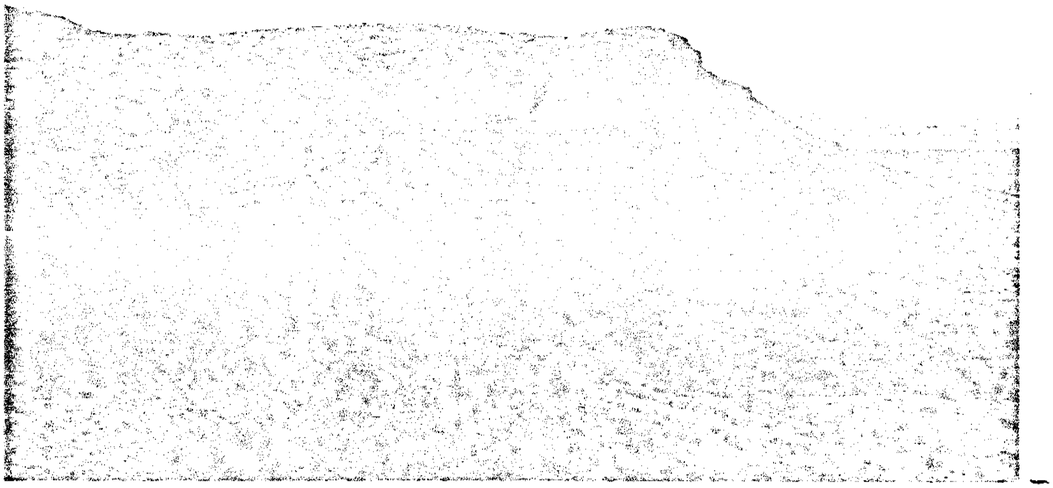

Fig. 23. Photo of fault within central canyon (arrow shows visible displacement).

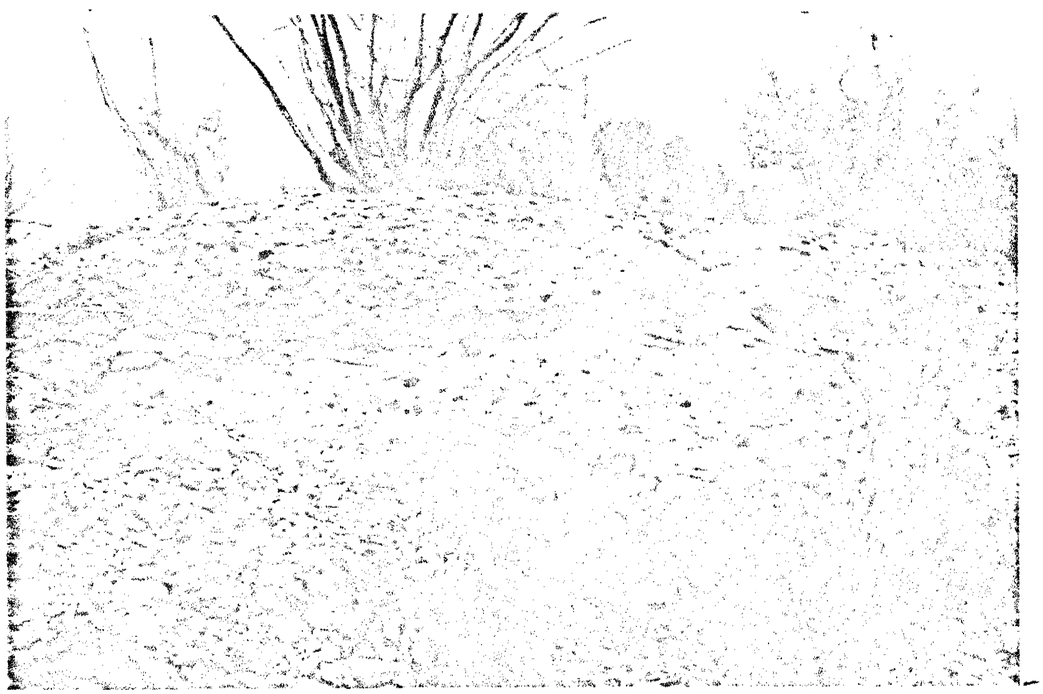

Fig. 24. Quaternary conglomerate cutting into Permian bioherm (not shown).

fault occurring between the breaks in the dikes the change in dip direction could have been caused by the lateral movement of the postulated fault. The timing of faulting is believed by Otte to be related to the Cenozoic deformation that created the Sacramento Mountains.

Conglomerates occur along the tops of the ridges in the area (Fig. 25). Otte (1959) believes these represent the remnants of a once continuous erosion surface that extended from the Yeso slope to the Tularosa Basin. The occurrence of these conglomerates 100 to 200 hundred feet (30.5 to 60.9 m) above the present erosion level gives evidence of the relative uplift between the mountain block and the valley block. The flat unwarped nature of these conglomerates suggest the uplift was caused by faulting rather than folding. Otte (1958) dates these conglomerates as

Conclusions

The interbedded carbonate and clastic sediments of the Laborcita Formation represent the effects of a fan-delta on a shallow marine shelf. Within this setting, periodic changes in the amount of clastic influx and the migration of the fan-delta lobes restricted the production and deposition of carbonate material.

Fan-delta deposits are recognized by the interfingering of coarse-grained clastics with finer shoreface clastics and shelf, lagoon and interdistributary bay carbonates. Only reworked distal fan-delta deposits are present within the study area. This is believed due to the small size of the study area. These are characterized by glauconitic (not X-Rayed), grain-supported conglomerates. The bases of these conglomerates show little signs of erosion and the elongate clasts are randomly oriented.

During times of negligible clastic influx, bioherms formed on the shallow shelf. The growth of the core occurred in three stages: 1) pioneer stage (Toomey and Cys, 1978); 2) growth stage; and 3) colonizing stage. The latter two stages are seen by the change in color from brownish-gray to light-gray. Along the top of the bioherm core, the presence of flanking and overlying back lagoonal beds indicate the progradation of the bioherm complex.

Development of the bioherm ended with the migration of prodelta shales into the area. This initiated a return to the cyclic changes between shelf and shoreface environments. Reestablishment of the fan-delta complex did not occur in the area.

Another bioherm developed at the top of the Laborcita Formation, but was not as extensive as the earlier one. The growth of this bioherm was likely influenced by the advance of the terrigenous Abo sands.

The only changes to occur in the area after the deposition of the Laborcita Formation were the intrusion of two Tertiary diabase dikes and uplift during the Quaternary. Two faults were created in the area as a result of this uplift. Conglomerates also formed during the Quaternary. These are found capping the hill tops behind the bioherm.

This type of geologic setting may have potential for hydrocarbon accumulation in the subsurface. Lagoonal and prodelta shales would provide the source rocks. Trapping mechanisms would be mostly structural, but the depositional and diagenetic history would also play an important role in the quality of the reservoir. The postulated subsurface bioherm to the west, seen by the lagoonal interpretation for one of the carbonate units, may represent one such reservoir rock.

In order to further establish the validity of the fan-delta model, the Laborcita Formation must be investigated to the east in an attempt to locate the main body of the fan-delta. It would also be interesting to determine the relationship between the clastics and carbonates to the west of the study area in order to find the postulated bioherm and better understand the final stages of the Oro Grande Basin. Both these studies would have to be done by examining drill cores. Another bioherm is present north of the study area. This bioherm is stratigraphically equivalent to the main bioherm in the study area. Differences between these bioherm are observed. The most noticeable is the lack of undulations along the color zones in the northern bioherm. It would be of interest to determine the cause of this difference and to see if any other differences exist.

Appendix A

Insoluble Residue

Preparation of Residue

Samples were collected from fresh outcrops at specific study localities. Sample locations are based on distances above and below a distinctive stratigraphic level. At each sample location, between 3 and 5 samples were collected for analysis.

Sample Preparation

Each sample was broken into fine-gravel and weighed to the nearest 0.01 gram. Three grams of each sample were put into a 250 ml beaker and placed under a hood.

Two solutions of Muriatic HCl were used, 10% and 15%. A small amount of 10% HCl was first poured on the sample. After the initial effervescence, 15% HCl was added. Care was taken to avoid the overflowing of effervescent material. Fresh 15% HCl was added until no visible reaction occured.

When no reaction was observed the spent acid and residue were poured onto weighed Whatman 5 Qualitative filter paper. The residue was washed thoroughly with distilled water and allowed to dry. To quicken drying the filter paper was placed in an oven. The oven was kept below 100 degree C.

The dried residue and filter paper were reweighed and the percent weight of insoluble residue determined. Insoluble residues were examined under binocular microscope. This was determined not to be of diagnostic value and not completed.

Data

Insoluble Residue

Color Changes

Northern Location

Sample Number	Sample Weight (gm)	Weight Filter Paper (gm)	Weight Residue + Filter paper (gm)	Weight Insoluble Residue (gm)	Weight Percent Insoluble Residue (gm)
I-A-1	15.45	1.34	1.62	0.28	1.81
I-A-2	15.19	1.24	1.70	0.46	3.03
I-A-3	16.49	1.24	1.84	0.60	3.64
I-B-1	16.53	1.33	1.71	0.38	2.30
I-B-2	15.02	1.28	1.51	0.23	1.53
I-B-3	16.01	1.23	1.42	0.19	1.19
I-B-4	15.75	1.28	1.52	0.24	1.52
I-C-1	16.38	1.33	1.45	0.12	0.73
I-C-2	16.45	1.27	1.59	0.32	1.94
I-C-4	15.35	1.34	1.45	0.11	0.72
I-D-1	15.99	1.24	1.34	0.10	0.62
I-D-2	15.45	1.19	1.34	0.15	0.97

I-D-3	15.79	1.31	1.46	0.15	0.95
I-D-4	15.67	1.34	1.48	0.12	0.77

Southern Location

Sample Number	Sample Weight (gm)	Weight Filter Paper (gm)	Weight Insoluble Residue + Filter Paper (gm)	Weight Insoluble Residue (gm)	Weight Percent Insoluble Residue (gm)
II-A-1	15.45	1.25	1.39	0.14	0.91
II-A-2	15.59	1.23	1.34	0.11	0.71
II-A-3	16.37	1.17	1.34	0.14	1.04
II-B-1	11.15	1.20	1.49	0.29	2.60
II-B-2	15.34	1.26	1.59	0.33	1.59
II-B-3	14.80	1.24	1.64	0.40	2.70
II-C-1	15.33	1.16	1.48	0.32	2.09
II-C-2	16.47	1.20	1.71	0.51	3.10
II-C-3	17.55	1.26	1.55	0.29	0.65
II-C-4	15.60	1.26	1.57	0.31	1.99
II-D-1	15.04	1.18	1.59	0.41	2.73
II-D-2	15.30	1.20	1.47	0.27	1.76
II-D-3	14.77	1.26	1.76	0.50	3.38
II-E-1	14.79	1.23	1.41	0.18	1.22
II-E-2	15.62	1.18	1.23	0.05	0.32
II-E-3	15.08	1.22	1.41	0.19	1.26

II-F-1	15.46	1.16	1.20	0.04	0.26
II-F-2	15.72	1.21	1.27	0.06	0.38
II-F-3	15.48	1.25	1.34	0.09	0.58
II-F-4	15.83	1.24	1.27	0.03	0.19

Bedding Changes

Sample Number	Sample Weight (gm)	Weight Filter Paper (gm)	Weight Insoluble Residue + Filter Paper (gm)	Weight Insoluble Residue (gm)	Weight % Insoluble Residue
III-A-1	16.26	1.27	1.54	0.27	1.66
III-A-2	15.99	1.16	1.36	0.20	1.25
III-A-3	15.77	1.30	1.70	0.40	2.54
III-A-4	15.40	1.29	1.50	0.21	1.36
III-B-1	15.77	1.23	1.72	0.49	3.11
III-B-2	15.85	1.17	1.43	0.26	1.64
III-B-3	17.04	1.31	1.70	0.39	2.29
III-B-4	15.74	1.23	1.63	0.40	2.54
III-C-1	15.69	1.26	1.88	0.62	3.95
III-C-2	17.03	1.16	1.41	0.25	1.48
III-C-3	15.99	1.28	1.58	0.30	1.88
III-C-4	16.84	1.25	1.79	0.54	3.21
III-D-1	16.12	1.27	1.89	0.62	3.85

Sample Number	Sample Weight (gm)	Weight Filter Paper (gm)	Weight Insoluble Residue + Filter Paper (gm)	Insoluble Residue (gm)	Weight % Insoluble Residue
III-D-2	15.73	1.15	1.99	0.84	5.34
III-D-3	15.75	1.30	1.32	0.02	0.13
III-D-4	15.84	1.24	1.53	0.29	1.83
III-E-1	16.55	1.38	1.49	0.11	0.66
III-E-2	16.24	1.15	1.47	0.32	1.97
III-E-3	16.23	1.23	1.49	0.26	1.60
III-E-4	16.24	1.25	1.48	0.23	1.42

Sample Number	Sample Weight (gm)	Weight Filter Paper (gm)	Weight Insoluble Residue + Filter Paper (gm)	Insoluble Residue (gm)	Weight % Insoluble Residue
IV-A-1	16.56	1.38	1.59	0.21	1.27
IV-A-2	15.77	1.22	1.42	0.20	1.27
IV-A-3	16.12	1.21	1.52	0.31	1.92
IV-A-4	16.88	1.21	1.50	0.29	1.72
IV-B-1	16.19	1.39	1.53	0.14	0.86
IV-B-2	16.21	1.23	1.43	0.20	1.23
IV-B-3	16.08	1.24	1.53	0.29	1.80
IV-C-1	16.41	1.14	1.47	0.33	2.01
IV-C-2	16.04	1.30	1.76	0.37	2.30
IV-C-3	16.54	1.26	1.78	0.52	3.14
IV-D-1	16.94	1.26	1.50	0.24	1.51
IV-D-2	16.44	1.25	1.46	0.21	1.28

IV-D-3	15.74	1.17	1.27	0.70	0.63
IV-D-4	15.58	1.22	1.28	0.06	0.38
IV-E-1	15.07	1.26	1.30	0.04	0.26
IV-E-2	15.95	1.23	1.37	0.14	0.88
IV-E-3	16.13	1.17	1.37	0.20	1.24
IV-E-4	17.11	1.19	1.73	0.54	3.16

Sample Number	Weight Sample Weight (gm)	Weight Filter Paper (gm)	Weight Insoluble Residue + Filter Paper (gm)	Insoluble Residue (gm)	Weight % Insoluble Residue
V-A-1	16.14	1.26	1.39	0.13	0.80
V-A-2	15.39	1.25	1.45	0.20	1.30
V-A-3	15.92	1.17	1.32	0.15	0.94
V-A-4	15.68	1.19	1.35	0.16	1.02
V-B-1	15.92	1.96	1.43	0.17	1.07
V-B-2	15.45	1.25	1.50	0.25	1.62
V-B-3	15.11	1.18	1.45	0.27	1.79
V-B-4	15.28	1.19	1.47	0.28	1.83
V-C-1	15.73	1.25	1.65	0.40	2.54
V-C-2	16.18	1.24	2.04	0.80	4.94
V-C-3	15.27	1.17	1.60	0.43	2.81
V-D-1	15.77	1.20	1.33	0.13	0.82
V-D-2	15.73	1.24	1.36	0.12	0.76

V-D-3	15.29	1.18	1.27	0.09	0.59
V-D-4	15.63	1.19	1.37	0.08	0.51
V-E-1	15.40	1.24	1.44	0.20	1.30
V-E-2	14.98	1.23	1.43	0.20	1.33
V-E-3	15.23	1.18	1.34	0.16	1.05
V-E-4	15.65	1.21	1.59	0.38	2.43

APPENDIX B

THIN SECTION DESCRIPTIONS

COLOR CHANGES

Study Location 2

Zone A: within the brownish-gray zone five feet (1.5 m) below the color change

Rock Name: after Dunham (1962): crystaline carbonate

Carbonate Constituents	Percent of Rock
Intraclasts:	none observed
Ooids:	none observed
Peloids: dark micrite circles with average diameter of 0.2 mm	trace
Skeletal Material: 1) phylloid algae, with micrite envelopes, interior filled with drusy and blocky spar; 2) crinoid columnals	trace
Micrite:	2 %
Neomorphic Spar: microspar with irregular line contacts, grades from micrite to pseudospar pseudospar with irregular and sutured contacts, average size 0.3 mm	53 %
Precipitated Spar: radial fans with average crystal lengths of 1.5 cm and widths of 0.15 mm, seen as ghost structures within neomorphic spar; blocky spar euhedral, average size 0.3 mm, found in algal moldic pores and associated with radial fans; syntaxial rim cement occurs on crinoids	30 %

Other Constituents

Terrigenous Material: opaque black and brown staining along crystal contacts 5 %

Organic Material: trace

Pore Space: fracture and dissolution pores 10 %

Zone B, three feet (0.9 m) below color contact

Rock Name: after Dunham (1962): mudstone

Carbonate Constituents	Percent of Rock
Intraclasts: rectangular to square dark micrite, average size 0.2 mm	2 %
Ooids: showing uniaxial extinction, average size 0.3 mm	trace
Peloids: irregular circles of micrite with no distinct boundaries, grade into neomorpic spar (pseudopeloids)	5 %
Skeletal Material: 1) ostracods with interparticle space filled with ppt. spar; 2) pelecypods with micrite envelopes interior dissolved and filled with ppt. spar; 3) foraminifera; 4) bryozoa; 5) echinoid spines; 6) phylloid algae wtih micrite envelopes, interior neomorphosed	10 %
Micrite:	50 %
Neomorphic Spar: microspar and pseudospar in gradational contact with micrite	8 %
Precipitated Spar: drusy and blocky spar with straight line contacts filling burrows, moldic and	

dissolution pores, drusy spar occurs along pore periphery 15 %

Other Constituents:

Terrigenous Material: Opaque euhedral crystals and specks believed to be iron occurs within ppt. spar 5 %

Organic Material: trace

Pore Space: fracture and dissolution pores 5 %

Zone C, within the light-gray zone, one foot (0.3 m) below color contact

Rock Name: after Dunham (1962): algal wackestone

Carbonate Constituents Percent of Rock

Intraclasts: none observed

Ooids: concentrically layered, uniaxial extinction, average diameter 0.3 mm trace

Pelloids: dark micrite circles, average diameter 0.2 mm trace

Skeletal Material: 1) phylloid algae, with micrite envelopes, interiors neomorphosed; 2) foraminifera; 3) bryozoa; 4) ostracods, interparticle space filled with ppt. spar; 5) gastropods with micrite envelopes, interior dissolved and filled with ppt. spar; 6) pelecypods with micrite envelopes, interior dissolved and filled with ppt. spar 15 %

Micrite: 35 %

Neomorphic Spar: microspar and pseudospar associated with micrite and replacing the interiors of algal blades 20 %

Precipitated Spar: drusy and blocky spar with straight line contacts filling moldic, shelter, dissolution and fracture pores 15 %

Other Constituents

Terrigeneous Material: opaque specks occuring within ppt spar, believed to be iron 5 %

Organic Material: trace

Pore Space: dissolution and fracture pores 10 %

Zone D, within the light-gray zone, one inch (2.56 cm) below the color contact

Rock Name: after Dunham (1962): fossiliferous packstone

Carbonate Constituents — Percent of Rock

Intraclasts: none observed

Ooids: elongate, concentrically layered circles with uniaxial extinction, average diameter 0.3 mm 1 %

Peloids: dark micrite circles, average diameter 0.15 mm trace

Skeletal Material: 1) bryozoa; 2) pelecypods, interiors dissolved and filled with ppt. spar; 3) gastropods, interiors dissolved and filled with ppt. spar; 4) ostracods; 5) crinoid columnals; 6) phylloid algae with micrite envelopes, interiors neomorphosed; 7) trilobite 35 %

Micrite: 25 %

Neomorphic Spar: microspar grading from micrite to pseudo-
spar with irregular contacts, replacing algal blade
interiors — 15 %

Precipitated Spar: drusy spar grading to blocky spar filling
burrows, moldic and interparticle pore space — 15 %

Other Constituents

Terrigeneous Material: opaque black and brown specks occurring
with ppt. spar, believed to be iron — 3 %

Organic Material: — trace

Pore Space: dissolution and fracture pores — 7 %

Zone E, within the brownish-gray zone, one inch (2.56 cm)
above the color contact

Rock Name: crystalline carbonate

Carbonate Constituents	Percent of Rock
Intraclasts: dark micrite rectangles, average size 0.3 mm	5 %
Ooids:	none observed
Pelloids:	none observed
Skeletal Material: 1) phylloid algae with micrite envelopes, interiors neomorphosed; 2) ostracods; 3) bryozoa; 4) crinoid columnals	5 %
Micrite:	7 %
Neomorphic Spar: microspar grading from micrite to pseudospar with irregular and sutured line contacts	38 %
Precipitated Spar: drusy spar grading into blocky spar with straight line contacts, filling shelter	

pores 30 %

Other Constituents

Terrigeneous Material: black opaque specks associated with ppt. spar 3 %

Organic Material: trace

Pore Space: dissolution pores 12 %

Zone F, within the brownish-gray zone, one foot (0.3 m) above the color contact

Rock Name: after Dunham (1962): crystaline carbonate

Carbonate Constituents	Percent of Rock
Intraclasts:	none observed
Ooids:	none observed
Peloids:	none observed
Skeletal Material: 1) phylloid algae with micrite envelopes, interiors neomorphosed, forming shelter pores; 2) crinoid columnal, being neomorphosed	10 %
Micrite:	8 %
Neomorphic Spar: microspar grading from micrite to pseudospar with irregular line contacts and an average size of 0.7mm	37 %
Precipitated Spar: radial fans filling shelter pores with an average length of 1.5 cm and width of 0.2 mm, seen as ghost structures within neomorphic spar	28 %

Other Constituents

Terrigeneous Material: brown staining occurring along crystal contacts 7 %

Organic Material: trace

Pore Space: dissolution and fracture pores 10 %

Bedding Change

Study Location 3

Zone A, one foot (0.3 m) below the black packstone

Rock Name: after Dunham (1962): fossiliferous wackestone

Carbonate Constituents	Percent of Rock
Intraclasts:	none observed
Ooids: concentrically layered circles with average diameter of 0.15 mm	trace
Peloids: dark micrite circles with 0.15 mm average diameter	1 %
Skeletal Material: 1) pelecypod with micrite envelopes, interiors dissolved and filled with ppt.spar; 2) foraminifera; 3) bryozoa; 4) gastropods with micrite envelopes, interior dissolved and filled with ppt. spar; 5) ostracods; 6) brachiopod spines; 7) crinoid columnals	10 %
Micrite:	70 %
Neomorphic Spar: microspar grades from micrite to pseudo-spar with irregular and sutured line contacts and 0.2 mm average size	5 %
Precipitated Spar: drusy spar grading to blocky spar filling burrows and moldic pores	7 %

Other Constituents

Terrigeneous Material: opaque mineral occurs as euhedral, irregular and circular bodies, average size 3 %

0.3 mm trace

Organic Material: 3 %

Pore Space: dissolution and fracture pores

Zone B, one inch (2.56 cm) below the black packstone

Rock Name: after Dunham (1962): mudstone

	Percent of Rock
Carbonate Constituents	
Intraclasts:	none observed
Ooids: elongate circles with radial extintion, average diameter 0.3 mm	trace
Peloids: micrite circles grade into neomorphic spar average diameter 0.2 mm (pseudopeloid)	2 %
Skeletal Material: 1) foraminifera; 2) pelecypods with micrite envelopes, interior dissolved and filled with ppt. spar; 3) bryozoa; 4) crinoid columnal, articulate	8 %
Micrite:	50 %
Neomorphic Spar: microspar grading from micrite to pseudospar with irregular line contacts, forms circular patches	16 %
Precipitated Spar: blocky spar with straight line contacts and 0.3 mm average size, filling moldic and dissolution pores	14 %

Other Constituents

Terrigeneous Material:	none observed
Organic Material:	trace
Pore Space: dissolution and fracture pores	10 %

Zone C, within the black packstone

Rock Name: after Dunham (1962): fossiliferous packstone

Carbonate Constituents	Percent of Rock
Intraclasts:	none observed
Ooids:	none observed
Peloids: dark micrite elipses, average diameter 0.2 mm	trace
Skeletal Material: 1) foraminifera; 2) crinoid columnals with micrite envelopes; 3) bryozoa; 4) pelecypods with micrite envelopes, interiors dissolved and filled with ppt. spar; 5) gastropods with micrite envelopes, interiors dissolved and filled with ppt. spar; 6) brachiopods; 7) ostracods	40 %
Micrite:	15 %
Neomorphic Spar: microspar occurring throughout associated with micrite	30 %
Precipitated Spar: drusy spar grading to blocky spar with straight line contacts, filling burrows and moldic pores	7 %

Other Constituents

Terrigeneous Material: opaque squares, specks and stain	1 %

Organic Material:	trace
Pore Space: dissolution pores	8 %

Zone D, one inch (2.56 mm) above the black packstone

Rock Name: after Dunham (1962): fossiliferous wackestone

Carbonate Constituents	Percent of Rock
Intraclasts:	none observed
Ooids:	none observed
Peloids: circular micrite bodies with 0.2 mm average diameter, edges grade into neomorphic spar (pseudopeloids)	5 %
Skeletal Material: 1) bryozoa; 2) blue-green algae forming laminations; 3) pelecypods with micrite envelopes, interiors dissolved and filled with ppt. spar; 4) brachiopods; 5) ostracods; crinoid columnals with syntaxial rim cement	20 %
Micrite:	15 %
Neomorphic Spar: microspar surrounding pseudopeloids	30 %
Precipitated Spar: drusy spar in sharp contact with micrite in burrows, grades into blocky spar, also filling moldic pores and shelter pores	20 %
Other Constituents	
Terrigeneous Material: opaque specks and euhedral crystals average diameter 0.2 mm	3 %
Organic Material:	trace
Pore Space: dissolution and intercrystaline pores	7 %

Zone E, one foot (0.3 m) above the black packstone

Rock Name: after Dunham (1962): fossiliferous wackestone

Carbonate Constituents	Percent of Rock
Intraclasts: dark rectangular micrite, 0.3 mm average diameter	1 %
Ooids: consentrically layered circles, 0.3 mm average diameter with uniaxial extinction	trace
Peloids: dark eliptical micrite bodies, 0.2 mm average diameter	2 %
Skeletal Material: 1) pelecypods with micrite envelopes, interiors dissolved and filled with ppt. spar; 2) bryozoa; 3) phylloid algae with micrite envelopes, interiors neomorphosed; 4) ostracods; 5) crinoid columnals, partially micritized; 6) trilobites	15 %
Micrite:	45 %
Neomorphic Spar: microspar occurs thoughout in gradational contact with micrite, locally grades into pseudospar with irregular line contacts, 0.2 mm average diameter	15 %
Precipitated Spar: drusy spar in sharp contact with micrite, grades into blocky spar with straight line contacts, 0.4 mm average diameter, occurs within burrows, moldic and interparticle pores	10 %
Other Constituents	
Terrigeneous Material: opaque specks with 0.1 mm average diameter	3 %

Organic Material:	trace
Pore Space: dissolution and fracture pores	9 %

Appendix C

Topographic Map

A topographic map was made to a scale of 1:1800 using a planetable and alidade. A twenty foot contour interval was used.

The base station was located at the corner marker for sections 16,17,20 and 21, T 14 S,R 10 E. The elevation of the base station was determined by using a Micro surveying altimeter that is accurate to +- 2 feet. The altimeter was standardized at the bench mark located at the base of the flag pole in front of the Administration Building for Tularosa School District No. 4.

Four hundred eighty one stations were shot, using nineteen planetable stations. The farthest distance shot was 1787 feet and greatest elevation change 221 feet. The error in closure was thirty three feet horizontally and ten feet vertically.

Aerial photographs were taken of the area using the same scale as the map. A mosaic of the area was made and assisted in drawing the contour lines.

REFERENCES

Allen, J. R. L., 1965, Late Quaternary Niger Delta, and Adjacent Areas: Sedimentary Environments and Lithofacies, Am. Assoc. Pet. Geol. Bull., v. 49, p. 547-600.

Bathurst, R. G. C., 1959, The Cavernous Structure of some Mississippian Stromatactis Reefs in Lancashire, England, Jour. Geol., v. 64, p. 506-521.

Burst, J. F., 1958, "Glauconite" Pellets: Their Mineral Native and Applications to Stratigraphic Interpretations, Am. Assoc. Pet. Geol. Bull, v. 42, no. 2, p. 310-327.

Compton, R. R., 1962, Manual of Field Geology, John Wiley & Sons, Inc., New York, 377 p.

Cys, J. M. and Mazzullo, S. J., Oct. 1977, Biohermal Submarine Cements Laborcita Formation (Permian), Northern Sacramento Mountains, New Mexico, in: Pray, L. C., Wilson, J. L., Toomey, D. F., leaders, Geology of the Sacramento Mountains, Otero County, New Mexico, Field Trip Guidebook, West Texas Geologic Society, p. 43-48.

Dunham, R. J., 1962, Classification of Carbonate Rocks according to Depositional Texture, p. 108-121 in: Ham, W. E., ed., Classification of Carbonate Rocks: Tulsa, Okla., Am. Assoc. Pet. Geol., Mem. 1, 279 p.

Dutton, S. P., 1982, Pennsylvanian Fan-Delta and Carbonate Deposition, Mobeetie Field, Texas Panhandle, Am. Assoc. Pet. Geol. Bull., v. 66, no. 4, p. 389-407.

Folk, R. L., 1968, Petrography of Sedimentary Rocks: Austin, Texas, Hemphill's Bookstore, 170 p.

Friedman, G. R., 1978, Principles of Sedimentation, John Wiley & Sons, Inc., New York, p. 301-306.

Galliher, E. W., 1935, Geology of Glauconite, Am. Assoc. Pet. Geol. Bull., v. 14, p. 1569-1601.

Galloway, W. E., 1976, Sediments and Stratigraphic Framework of the Copper River Fan-Delta, Alaska, Jour. Sed. Pet., v. 46, no. 3, p. 726-737.

Ginsburg, R., Rezak, R., and Wray, J. L., 1972, Geology of Calcareous Algae: Univ. Miami Short Course Lecture Notes, Comparative Sedimentology Laboratory, Div. Marine Geology and Geophysics, Univ. Miami, Miami, Florida.

Handford, C. R., and Dutton, S. P., 1980, Pennsylvanian-Early Permian Depositional Systems and Shelf-Margin Evolution, Palo Duro Basin, Texas, Am. Assoc. Pet. Geol. Bull, v. 64, no. 1, p. 88-106.

Harms, J. C., 1969, Hydraulic Significance of some Sand Ripples, Geol. Soc. Am. Bull., v. 80, p. 363-396.

Heckal, P. H., 1972, Recognition of Ancient Shallow Marine Environments, p. 226-286, in: Rigby, J. K., and Hamblin, W. K., eds., Recognition of Ancient Sedimentary Environments: Tulsa, Okla., Soc. Econ. Paleontologists and Mineralogists, Spec. Pub. No. 16, 340 p.

oward, J. D., and Reineck, H. E., 1972, Georgia Coastal Region, Sapelo Island, U.S.A.: Sedimentology and Biology, VII, Conclusions: Senckenbargiana Martima, v. 4, p. 217-222.

ottlowksi, F. E., 1963, Paleozoic and Mesozoic Strata of Southwestern and South-Central New Mexico, New Mexico Inst. of Min. and Tech., State Bur. of Mines and Min. Res. Bull. 79, 100 p.

ogan, B. W., Rezak, R., and Ginsburg, R. N., 1964, Classification and Environmental Significance of Algal Stromatolites: Jour. Geol. v. 72, p. 68-83.

ongman, M. W., 1980, Carbonate Diagenetic Textures from Near Surface Diagenetic Environments, Am. Assoc. Pet. Geol. Bull., v. 64, no. 4, p. 461-489.

cGowen, J. H., 1970, Gum Hollow Fan Delta, Nueces Bay, Texas: Texas Univ. Bur. Econ. Geology Rept. Inv. 69, 91 p.

oore, 1957, Modern Methods of Paleoecology, Am. Assoc. Pet. Geol. Bull., v. 41, p. 1787-1788.

ewell, W. D., Imbrie, J., Purdy, E. G., Thurber, D. T., 1959, Organism Communities and Bottom Facies, Great Bahama Banks: Am. Mus. Nat. Hist. Bull., v. 117, p. 117-228.

tte, C. J., 1959, Late Pennsylvanian and Early Permian Stratigraphy of the Northern Sacramento Mountians, Otero County, New Mexico: New Mexico Bur. Mines and Mineral Res. Bull. 50, 111 p.

tte, C. J., and Parks, J. M., Jr., 1963, Fabric Studies of Virgil and Wolfcamp Bioherms, New Mexico, Jour. of Geol., v. 71, p. 380-396.

:renga, D. H., 1967, Glauconite and Chamosite as Depth Indicators in the Marine Environment, Marine Geology, p. 495-501.

Pray, L. C., 1961, Geology of the Sacramento Mountains Escarpment, Otero County, New Mexico: New Mexico Bur. Mines and Mineral Res. Bull. 35, 143 p.

Reinek, H. E., and Singh, I. B., 1975, Depositonal Sedimentary Environments, Springer-Verlag, New York, 439 p.

Ruchin, L. B., 1958, Grundzuge der Lithologie, Berlin: Akademic-Verlag, 806 p.

Strangway, D. W., 1970, History of the Earth's Magnetic Field, McGraw-Hill Pub. Co., New York, 168 p.

rry, R. D., and Chilingar, G. V., 1955, Summary of "Concerning some Additonal Aids in Studing Sedimentary Formations", Jour. Sed. Pet., v. 25, p. 229-234.

Toomey, D. F. and Cys, J. M., 1979, Community Succession in Small Bioherms of Algae and Sponges in the Lower Permian of New Mexico, Lathaia, v. 12, p. 65-74.

Triplehorn, D. M., 1966, Glauconite Provides Good Oil Search Date, World Oil, v. 162, p. 94-97.

Van Houten, F. B., 1964, Origin of Red Beds - Some Unsolved Problems; p. 647-661, in Nairn, A. E. M., ed., Problems in Peleoclimatology, Interscience Publishers, New York.

Walpole, R. E. and Myers, R. H., 1978, Probability and Statistics for Engineers and Scientists, 2nd ed., MacMillan Publishing Co., Inc., Chapter 13, p. 473-495.

Wentworth, C. K., 1922, A Scale of Grade and Class Terms for Clastic Sediments, Jour. Geol., v. 30, p. 377-392.

escott, W. A. and Ethridge, F. G., 1980, Fan-Delta Sedimentology and Tectonic Setting - Yallahs Fan Delta, Southeast Jamaica, Am. Assoc. Pet. Geol. Bull, v. 64, no. 3, p. 374-399.

ilson, J. L., 1967, Cyclic and Reciprocal Sedimentation in Virgilian Strata of Southern New Mexico, Geol. Soc. Am. Bull., v. 78, p. 805-818.

ilson, J. L., 1975, Carbonate Facies in Geologic History: New York, Springer-Verlag, 471 p.